

Projection Robust Wasserstein Distance and Riemannian Optimization

Tianyi Lin^{*,◦} Chenyou Fan^{*,◦,□} Nhat Ho[‡] Marco Cuturi^{△,▷} Michael I. Jordan^{◦,†}

Department of Electrical Engineering and Computer Sciences[◦]

Department of Statistics[†]

University of California, Berkeley

The Chinese University of Hong Kong, Shenzhen[□]

Department of Statistics and Data Sciences, University of Texas, Austin[‡]

CREST - ENSAE[△], Google Brain[▷]

May 4, 2022

Abstract

Projection robust Wasserstein (PRW) distance, or Wasserstein projection pursuit (WPP), is a robust variant of the Wasserstein distance. Recent work suggests that this quantity is more robust than the standard Wasserstein distance, in particular when comparing probability measures in high-dimensions. However, it is ruled out for practical application because the optimization model is essentially non-convex and non-smooth which makes the computation intractable. Our contribution in this paper is to revisit the original motivation behind WPP/PRW, but take the hard route of showing that, despite its non-convexity and lack of nonsmoothness, and even despite some hardness results proved by [Niles-Weed and Rigollet \[2019\]](#) in a minimax sense, the original formulation for PRW/WPP *can* be efficiently computed in practice using Riemannian optimization, yielding in relevant cases better behavior than its convex relaxation. More specifically, we provide three simple algorithms with solid theoretical guarantee on their complexity bound (one in the appendix), and demonstrate their effectiveness and efficiency by conducting extensive experiments on synthetic and real data. This paper provides a first step into a computational theory of the PRW distance and provides the links between optimal transport and Riemannian optimization.

1 Introduction

Optimal transport (OT) theory [[Villani, 2003, 2008](#)] has become an important source of ideas and algorithmic tools in machine learning and related fields. Examples include contributions to generative modelling [[Arjovsky et al., 2017](#), [Salimans et al., 2018](#), [Genevay et al., 2018a](#), [Tolstikhin et al., 2018](#), [Genevay et al., 2018b](#)], domain adaptation [[Courty et al., 2017](#)], clustering [[Srivastava et al., 2015](#), [Ho et al., 2017](#)], dictionary learning [[Rolet et al., 2016](#), [Schmitz et al., 2018](#)], text mining [[Lin et al., 2019c](#)], neuroimaging [[Janati et al. \[2020\]](#)] and single-cell genomics [[Schiebinger et al., 2019](#), [Yang et al., 2020](#)]. The Wasserstein geometry has also provided a simple and useful analytical tool to study latent mixture models [[Ho and Nguyen, 2016](#)], reinforcement learning [[Bellemare et al., 2017](#)], sampling [[Cheng et al., 2018](#), [Dalalyan and Karagulyan, 2019](#), [Mou et al., 2019](#), [Bernton, 2018](#)] and stochastic optimization [[Nagaraj et al., 2019](#)]. For an overview of OT theory and the relevant applications, we refer to the recent survey [[Peyré and Cuturi, 2019](#)].

^{*} Tianyi Lin and Chenyou Fan contributed equally to this work.

[◦] Chenyou Fan contributed during working at Google.

Curse of Dimensionality in OT. A significant barrier to the direct application of OT in machine learning lies in some inherent statistical limitations. It is well known that the sample complexity of approximating Wasserstein distances between densities using only samples can grow exponentially in dimension [Dudley, 1969, Fournier and Guillin, 2015, Weed and Bach, 2019, Lei, 2020]. Practitioners have long been aware of this issue of the curse of dimensionality in applications of OT, and it can be argued that most of the efficient computational schemes that are known to improve computational complexity also carry out, implicitly through their simplifications, some form of statistical regularization. There have been many attempts to mitigate this curse when using OT, whether through entropic regularization [Cuturi, 2013, Cuturi and Doucet, 2014, Genevay et al., 2019, Mena and Niles-Weed, 2019]; other regularizations [Dessein et al., 2018, Blondel et al., 2018]; quantization [Canas and Rosasco, 2012, Forrow et al., 2019]; simplification of the dual problem in the case of 1-Wasserstein distance [Shirdhonkar and Jacobs, 2008, Arjovsky et al., 2017] or by only using second-order moments of measures to fall back on the Bures-Wasserstein distance [Bhatia et al., 2018, Muzellec and Cuturi, 2018, Chen et al., 2018].

Subspace projections: PRW and WPP. We focus in this paper on another important approach to regularize the Wasserstein distance: Project input measures onto lower-dimensional subspaces and compute the Wasserstein distance between these reductions, instead of the original measures. The simplest and most representative example of this approach is the sliced Wasserstein distance [Rabin et al., 2011, Bonneel et al., 2015, Kolouri et al., 2019, Nguyen et al., 2020], which is defined as the average Wasserstein distance obtained between random 1D projections. In an important extension, Paty and Cuturi [2019] and Niles-Weed and Rigollet [2019] proposed very recently to look for the k -dimensional subspace ($k > 1$) that would maximize the Wasserstein distance between two measures after projection. [Paty and Cuturi, 2019] called that quantity the *projection robust Wasserstein* (PRW) distance, while [Niles-Weed and Rigollet, 2019] named it *Wasserstein Projection Pursuit* (WPP). PRW/WPP are conceptually simple, easy to interpret, and do solve the curse of dimensionality in the so called spiked model as proved in [Niles-Weed and Rigollet, 2019, Theorem 1] by recovering an optimal $1/\sqrt{n}$ rate. Very recently, Lin et al. [2020] further provided several fundamental statistical bounds for PRW as well as asymptotic guarantees for learning generative models with PRW. Despite this appeal, [Paty and Cuturi, 2019] quickly rule out PRW for practical applications because it is non-convex, and fall back on a convex relaxation, called the *subspace robust Wasserstein* (SRW) distance, which is shown to work better empirically than the usual Wasserstein distance. Similarly, [Niles-Weed and Rigollet, 2019] seem to lose hope that it can be computed, by stating “*it is unclear how to implement WPP efficiently*,” and after having proved positive results on sample complexity, conclude their paper on a negative note, showing hardness results which apply for WPP when the ground cost is the Euclidean metric (the 1-Wasserstein case). Our contribution in this paper is to revisit the original motivation behind WPP/PRW, but take the hard route of showing that, despite its non-convexity and lack of nonsmoothness, and even despite some hardness results proved in Niles-Weed and Rigollet [2019] in a minimax sense, the original formulation for PRW/WPP *can* be efficiently computed in practice using Riemannian optimization, yielding in relevant cases better behavior than SRW. For simplicity, we refer from now on to PRW/WPP as PRW.

Contribution: In this paper, we study the computation of the PRW distance between two discrete probability measures of size n . We show that the resulting optimization problem has a special structure, allowing it to be solved in an efficient manner using Riemannian optimization [Absil et al., 2009, Boumal et al., 2019, Kasai et al., 2019, Chen et al., 2020]. Our contributions can be summarized as follows.

1. We propose a max-min optimization model for computing the PRW distance. The maximization and minimization are performed over the Stiefel manifold and the transportation polytope, respectively. We prove the existence of the subdifferential (Lemma 2.3), which allows us to properly define an ϵ -approximate pair of optimal subspace projection and optimal transportation plan (Definition 2.7) and carry out a finite-time analysis of the algorithm.
2. We define an entropic regularized PRW distance between two finite discrete probability measures, and show that it is possible to efficiently optimize this distance over the transportation polytope using the Sinkhorn iteration. This poses the problem of performing the maximization over the Stiefel manifold, which is not solvable by existing optimal transport algorithms [Cuturi, 2013, Altschuler et al., 2017, Dvurechensky et al., 2018, Lin et al., 2019a,b, Guminov et al., 2019]. To this end, we propose two new algorithms, which we refer to as *Riemannian gradient ascent with Sinkhorn* (RGAS) and *Riemannian adaptive gradient ascent with Sinkhorn* (RAGAS), for computing the entropic regularized PRW distance. These two algorithms are guaranteed to return an ϵ -approximate pair of optimal subspace projection and optimal transportation plan with a complexity bound of $\tilde{O}(n^2 d \epsilon^{-6} + n^2 \epsilon^{-10})$. To the best of our knowledge, our algorithms are the first provably efficient algorithms for the computation of the PRW distance.
3. We provide comprehensive empirical studies to evaluate our algorithms on synthetic and real datasets. Experimental results confirm our conjecture that the PRW distance performs better than its convex relaxation counterpart, the SRW distance. Moreover, we show that the RGAS and RAGAS algorithms are faster than the Frank-Wolfe algorithm while the RAGAS algorithm is more robust than the RGAS algorithm.

Organization. The remainder of the paper is organized as follows. In Section 2, we present the nonconvex max-min optimization model for computing the PRW distance and its entropic regularized version. We also briefly summarize various concepts of geometry and optimization over the Stiefel manifold. In Section 3, we propose and analyze the RGAS and RAGAS algorithms for computing the entropic regularized PRW distance and prove that both algorithms achieve the finite-time guarantee under stationarity measure. In Section 4, we conduct extensive experiments on both synthetic and real datasets, demonstrating that the PRW distance provides a computational advantage over the SRW distance in real application problems. In the supplementary material, we provide further background materials on Riemannian optimization, experiments with the algorithms, and proofs for key results. For the sake of completeness, we derive a near-optimality condition (Definition B.1 and B.2) for the max-min optimization model and propose another *Riemannian SuperGradient Ascent with Network simplex iteration* (RSGAN) algorithm for computing the PRW distance without regularization and prove the finite-time convergence under the near-optimality condition.

Notation. We let $[n]$ be the set $\{1, 2, \dots, n\}$ and \mathbb{R}_+^n be the set of all vectors in \mathbb{R}^n with nonnegative components. $\mathbf{1}_n$ and $\mathbf{0}_n$ are the n -dimensional vectors of ones and zeros. $\Delta^n = \{u \in \mathbb{R}_+^n : \mathbf{1}_n^\top u = 1\}$ is the probability simplex. For a vector $x \in \mathbb{R}^n$, the Euclidean norm stands for $\|x\|$ and the Dirac delta function at x stands for $\delta_x(\cdot)$. The notation $\text{Diag}(x)$ denotes an $n \times n$ diagonal matrix with x as the diagonal elements. For a matrix $X \in \mathbb{R}^{n \times n}$, the right and left marginals are denoted $r(X) = X\mathbf{1}_n$ and $c(X) = X^\top \mathbf{1}_n$, and $\|X\|_\infty = \max_{1 \leq i, j \leq n} |X_{ij}|$ and $\|X\|_1 = \sum_{1 \leq i, j \leq n} |X_{ij}|$. The notation $\text{diag}(X)$ stands for an n -dimensional vector which corresponds to the diagonal elements of X . If X is symmetric, $\lambda_{\max}(X)$ stands for largest eigenvalue. The notation $\text{St}(d, k) := \{X \in \mathbb{R}^{d \times k} : X^\top X = I_k\}$ denotes the

Stiefel manifold. For $X, Y \in \mathbb{R}^{n \times n}$, we denote $\langle X, Y \rangle = \text{Trace}(X^\top Y)$ as the Euclidean inner product and $\|X\|_F$ as the Frobenius norm of X . We let $P_{\mathcal{S}}$ be the orthogonal projection onto a closed set \mathcal{S} and $\text{dist}(X, \mathcal{S}) = \inf_{Y \in \mathcal{S}} \|X - Y\|_F$ denotes the distance between X and \mathcal{S} . Lastly, $a = O(b(n, d, \epsilon))$ stands for the upper bound $a \leq C \cdot b(n, d, \epsilon)$ where $C > 0$ is independent of n and $1/\epsilon$ and $a = \tilde{O}(b(n, d, \epsilon))$ indicates the same inequality where C depends on the logarithmic factors of n , d and $1/\epsilon$.

2 Projection Robust Wasserstein Distance

In this section, we present the basic setup and optimality conditions for the computation of the projection robust 2-Wasserstein (PRW) distance between two discrete probability measures with at most n components. We also review basic ideas in Riemannian optimization.

2.1 Structured max-min optimization model

In this section we define the PRW distance [Paty and Cuturi, 2019] and show that computing the PRW distance between two discrete probability measures supported on at most n points reduces to solving a structured max-min optimization model over the Stiefel manifold and the transportation polytope.

Let $\mathcal{P}(\mathbb{R}^d)$ be the set of Borel probability measures in \mathbb{R}^d and let $\mathcal{P}_2(\mathbb{R}^d)$ be the subset of $\mathcal{P}(\mathbb{R}^d)$ consisting of probability measures that have finite second moments. Let $\mu, \nu \in \mathcal{P}_2(\mathbb{R}^d)$ and $\Pi(\mu, \nu)$ be the set of couplings between μ and ν . The 2-Wasserstein distance [Villani, 2008] is defined by

$$\mathcal{W}_2(\mu, \nu) := \left(\inf_{\pi \in \Pi(\mu, \nu)} \int \|x - y\|^2 d\pi(x, y) \right)^{1/2}.$$

To define the PRW distance, we require the notion of the push-forward of a measure by an operator. Letting $\mathcal{X}, \mathcal{Y} \subseteq \mathbb{R}^d$ and $T : \mathcal{X} \rightarrow \mathcal{Y}$, the push-forward of $\mu \in \mathcal{P}(\mathcal{X})$ by T is defined by $T_\# \mu \in \mathcal{P}(\mathcal{Y})$. In other words, $T_\# \mu$ is the measure satisfying $T_\# \mu(A) = \mu(T^{-1}(A))$ for any Borel set in \mathcal{Y} .

Definition 2.1 For $\mu, \nu \in \mathcal{P}_2(\mathbb{R}^d)$, let $\mathcal{G}_k = \{E \subseteq \mathbb{R}^d \mid \dim(E) = k\}$ be the Grassmannian of k -dimensional subspace of \mathbb{R}^d and let P_E be the orthogonal projector onto E for all $E \in \mathcal{G}_k$. The k -dimensional PRW distance is defined as $\mathcal{P}_k(\mu, \nu) := \sup_{E \in \mathcal{G}_k} \mathcal{W}_2(P_E \# \mu, P_E \# \nu)$.

Paty and Cuturi [2019, Proposition 5] have shown that there exists a subspace $E^* \in \mathcal{G}_k$ such that $\mathcal{P}_k(\mu, \nu) = \mathcal{W}_2(P_{E^*} \# \mu, P_{E^*} \# \nu)$ for any $k \in [d]$ and $\mu, \nu \in \mathcal{P}_2(\mathbb{R}^d)$. For any $E \in \mathcal{G}_k$, the mapping $\pi \mapsto \int \|P_E(x - y)\|^2 d\pi(x, y)$ is lower semi-continuous. This together with the compactness of $\Pi(\mu, \nu)$ implies that the infimum is a minimum. Therefore, we obtain a structured max-min optimization problem:

$$\mathcal{P}_k(\mu, \nu) = \max_{E \in \mathcal{G}_k} \min_{\pi \in \Pi(\mu, \nu)} \left(\int \|P_E(x - y)\|^2 d\pi(x, y) \right)^{1/2}.$$

Let us now consider this general problem in the case of discrete probability measures, which is the focus of the current paper. Let $\{x_1, x_2, \dots, x_n\} \subseteq \mathbb{R}^d$ and $\{y_1, y_2, \dots, y_n\} \subseteq \mathbb{R}^d$ denote sets of n atoms, and let $(r_1, r_2, \dots, r_n) \in \Delta^n$ and $(c_1, c_2, \dots, c_n) \in \Delta^n$ denote weight vectors. We define discrete probability measures $\mu := \sum_{i=1}^n r_i \delta_{x_i}$ and $\nu := \sum_{j=1}^n c_j \delta_{y_j}$. In this setting, the computation of the k -dimensional PRW distance between μ and ν reduces to solving a structured max-min optimization model where the maximization and minimization are performed over the Stiefel manifold $\text{St}(d, k) := \{U \in \mathbb{R}^{d \times k} \mid U^\top U =$

Algorithm 1 Riemannian Gradient Ascent with Sinkhorn Iteration (RGAS)

- 1: **Input:** $\{(x_i, r_i)\}_{i \in [n]}$ and $\{(y_j, c_j)\}_{j \in [n]}$, $k = \tilde{O}(1)$, $U_0 \in \text{St}(d, k)$ and ϵ .
- 2: **Initialize:** $\hat{\epsilon} \leftarrow \min\{\epsilon, \frac{\epsilon^2}{500\|C\|_\infty}\}$, $\eta \leftarrow \frac{\hat{\epsilon}}{4\log(n)}$ and $\gamma \leftarrow \frac{1}{(8L_1^2 + 16L_2)\|C\|_\infty + 16\eta^{-1}L_1^2\|C\|_\infty^2}$.
- 3: **for** $t = 0, 1, 2, \dots$ **do**
- 4: Compute $\pi_{t+1} \leftarrow \text{REGOT}(\{(x_i, r_i)\}_{i \in [n]}, \{(y_j, c_j)\}_{j \in [n]}, U_t, \eta, \hat{\epsilon})$.
- 5: Compute $\xi_{t+1} \leftarrow P_{\text{Tr}_{U_t} \text{St}}(2V_{\pi_{t+1}} U_t)$.
- 6: Compute $U_{t+1} \leftarrow \text{Retr}_{U_t}(\gamma \xi_{t+1})$.
- 7: **end for**

$I_k\}$ and the transportation polytope $\Pi(\mu, \nu) := \{\pi \in \mathbb{R}_+^{n \times n} \mid r(\pi) = r, c(\pi) = c\}$ respectively. Formally, we have

$$\max_{U \in \mathbb{R}^{d \times k}} \min_{\pi \in \mathbb{R}_+^{n \times n}} \sum_{i=1}^n \sum_{j=1}^n \pi_{i,j} \|U^\top x_i - U^\top y_j\|^2 \quad \text{s.t. } U^\top U = I_k, \quad r(\pi) = r, \quad c(\pi) = c. \quad (2.1)$$

The computation of this PRW distance raises numerous challenges. Indeed, there is no guarantee for finding a global Nash equilibrium as the special case of nonconvex optimization is already NP-hard [Murty and Kabadi, 1987]; moreover, Sion's minimax theorem [Sion, 1958] is not applicable here due to the lack of quasi-convex-concave structure. More practically, solving Eq. (2.1) is expensive since (i) preserving the orthogonality constraint requires the singular value decompositions (SVDs) of a $d \times d$ matrix, and (ii) projecting onto the transportation polytope results in a costly quadratic network flow problem. To avoid this, [Paty and Cuturi, 2019] proposed a convex surrogate for Eq. (2.1):

$$\max_{0 \preceq \Omega \preceq I_d} \min_{\pi \in \mathbb{R}_+^{n \times n}} \sum_{i=1}^n \sum_{j=1}^n \pi_{i,j} (x_i - y_j)^\top \Omega (x_i - y_j), \quad \text{s.t. } \text{Trace}(\Omega) = k, \quad r(\pi) = r, \quad c(\pi) = c. \quad (2.2)$$

Eq. (2.2) is intrinsically a bilinear minimax optimization model which makes the computation tractable. Indeed, the constraint set $\mathcal{R} = \{\Omega \in \mathbb{R}^{d \times d} \mid 0 \preceq \Omega \preceq I_d, \text{Trace}(\Omega) = k\}$ is convex and the objective function is bilinear since it can be rewritten as $\langle \Omega, \sum_{i=1}^n \sum_{j=1}^n \pi_{i,j} (x_i - y_j) (x_i - y_j)^\top \rangle$. Eq. (2.2) is, however, only a convex relaxation of Eq. (2.1) and its solutions are not necessarily good approximate solutions for the original problem. Moreover, the existing algorithms for solving Eq. (2.2) are also unsatisfactory—in each loop, we need to solve a OT or entropic regularized OT exactly and project a $d \times d$ matrix onto the set \mathcal{R} using the SVD decomposition, both of which are computationally expensive as d increases (see Algorithm 1 and 2 in Paty and Cuturi [2019]).

2.2 Entropic regularized projection robust Wasserstein

Eq. (2.1) has structure that can be exploited. Indeed, fixing a $U \in \text{St}(d, k)$, the problem reduces to minimizing a linear function over the transportation polytope, i.e., the OT problem. Therefore, we can reformulate Eq. (2.1) as the maximization of the function $f(U) := \min_{\pi \in \Pi(\mu, \nu)} \sum_{i=1}^n \sum_{j=1}^n \pi_{i,j} \|U^\top x_i - U^\top y_j\|^2$ over the Stiefel manifold $\text{St}(d, k)$.

Since the OT problem admits multiple optimal solutions, f is not differentiable which makes the optimization over the Stiefel manifold hard [Absil and Hosseini, 2019]. Computations are greatly facilitated by adding smoothness, which allows the use of gradient-type and adaptive gradient-type algorithms.

This inspires us to consider an entropic regularized version of Eq. (2.1), where an entropy penalty is added to the PRW distance. The resulting optimization model is as follows:

$$\max_{U \in \mathbb{R}^{d \times k}} \min_{\pi \in \mathbb{R}_+^{n \times n}} \sum_{i=1}^n \sum_{j=1}^n \pi_{i,j} \|U^\top x_i - U^\top y_j\|^2 - \eta H(\pi) \quad \text{s.t. } U^\top U = I_k, \quad r(\pi) = r, \quad c(\pi) = c, \quad (2.3)$$

where $\eta > 0$ is the regularization parameter and $H(\pi) := -\langle \pi, \log(\pi) - \mathbf{1}_n \mathbf{1}_n^\top \rangle$ denotes the entropic regularization term. We refer to Eq. (2.3) as the computation of *entropic regularized PRW distance*. Accordingly, we define the function $f_\eta = \min_{\pi \in \Pi(\mu, \nu)} \{\sum_{i=1}^n \sum_{j=1}^n \pi_{i,j} \|U^\top x_i - U^\top y_j\|^2 - \eta H(\pi)\}$ and reformulate Eq. (2.3) as the maximization of the differentiable function f_η over the Stiefel manifold $\text{St}(d, k)$. Indeed, for any $U \in \text{St}(d, k)$ and a fixed $\eta > 0$, there exists a unique solution $\pi^* \in \Pi(\mu, \nu)$ such that $\pi \mapsto \sum_{i=1}^n \sum_{j=1}^n \pi_{i,j} \|U^\top x_i - U^\top y_j\|^2 - \eta H(\pi)$ is minimized at π^* . When η is large, the optimal value of Eq. (2.3) may yield a poor approximation of Eq. (2.1). To guarantee a good approximation, we scale the regularization parameter η as a function of the desired accuracy of the approximation. Formally, we consider the following relaxed optimality condition for $\hat{\pi} \in \Pi(\mu, \nu)$ given $U \in \text{St}(d, k)$.

Definition 2.2 *The transportation plan $\hat{\pi} \in \Pi(\mu, \nu)$ is called an ϵ -approximate optimal transportation plan for a given $U \in \text{St}(d, k)$ if the following inequality holds:*

$$\sum_{i=1}^n \sum_{j=1}^n \hat{\pi}_{i,j} \|U^\top x_i - U^\top y_j\|^2 \leq \min_{\pi \in \Pi(\mu, \nu)} \sum_{i=1}^n \sum_{j=1}^n \pi_{i,j} \|U^\top x_i - U^\top y_j\|^2 + \epsilon.$$

2.3 Optimality condition

Recall that the computation of the PRW distance in Eq. (2.1) and the entropic regularized PRW distance in Eq. (2.3) are equivalent to

$$\max_{U \in \text{St}(d, k)} \left\{ f(U) := \min_{\pi \in \Pi(\mu, \nu)} \sum_{i=1}^n \sum_{j=1}^n \pi_{i,j} \|U^\top x_i - U^\top y_j\|^2 \right\}, \quad (2.4)$$

and

$$\max_{U \in \text{St}(d, k)} \left\{ f_\eta(U) := \min_{\pi \in \Pi(\mu, \nu)} \sum_{i=1}^n \sum_{j=1}^n \pi_{i,j} \|U^\top x_i - U^\top y_j\|^2 - \eta H(\pi) \right\}. \quad (2.5)$$

Since $\text{St}(d, k)$ is a compact matrix submanifold of $\mathbb{R}^{d \times k}$ [Boothby, 1986], Eq. (2.4) and Eq. (2.5) are both special instances of the Stiefel manifold optimization problem. The dimension of $\text{St}(d, k)$ is equal to $dk - k(k+1)/2$ and the tangent space at the point $Z \in \text{St}(d, k)$ is defined by $T_Z \text{St} := \{\xi \in \mathbb{R}^{d \times k} : \xi^\top Z + Z^\top \xi = 0\}$. We endow $\text{St}(d, k)$ with Riemannian metric inherited from the Euclidean inner product $\langle X, Y \rangle$ for any $X, Y \in T_Z \text{St}$ and $Z \in \text{St}(d, k)$. Then the projection of $G \in \mathbb{R}^{d \times k}$ onto $T_Z \text{St}$ is given by Absil et al. [2009, Example 3.6.2]: $P_{T_Z \text{St}}(G) = G - Z(G^\top Z + Z^\top G)/2$. We make use of the notion of a *retraction*, which is the first-order approximation of an exponential mapping on the manifold and which is amenable to computation [Absil et al., 2009, Definition 4.1.1]. For the Stiefel manifold, we have the following definition:

Definition 2.3 A retraction on $\text{St} \equiv \text{St}(d, k)$ is a smooth mapping $\text{Retr} : \text{TSt} \rightarrow \text{St}$ from the tangent bundle TSt onto St such that the restriction of Retr onto $\text{T}_Z \text{St}$, denoted by Retr_Z , satisfies that (i) $\text{Retr}_Z(0) = Z$ for all $Z \in \text{St}$ where 0 denotes the zero element of TSt , and (ii) for any $Z \in \text{St}$, it holds that $\lim_{\xi \in \text{T}_Z \text{St}, \xi \rightarrow 0} \|\text{Retr}_Z(\xi) - (Z + \xi)\|_F / \|\xi\|_F = 0$.

The retraction on the Stiefel manifold has the following well-known properties [Boumal et al., 2019, Liu et al., 2019] which are important to subsequent analysis in this paper.

Proposition 2.1 For all $Z \in \text{St} \equiv \text{St}(d, k)$ and $\xi \in \text{T}_Z \text{St}$, there exist constants $L_1 > 0$ and $L_2 > 0$ such that the following two inequalities hold:

$$\begin{aligned} \|\text{Retr}_Z(\xi) - Z\|_F &\leq L_1 \|\xi\|_F, \\ \|\text{Retr}_Z(\xi) - (Z + \xi)\|_F &\leq L_2 \|\xi\|_F^2. \end{aligned}$$

For the sake of completeness, we provide four popular restrictions [Edelman et al., 1998, Wen and Yin, 2013, Liu et al., 2019, Chen et al., 2020] on the Stiefel manifold in practice. Determining which one is the most efficient in the algorithm is still an open question; see the discussion after Liu et al. [2019, Theorem 3] or before Chen et al. [2020, Fact 3.6].

- **Exponential mapping.** It takes $8dk^2 + O(k^3)$ flops and has the closed-form expression:

$$\text{Retr}_Z^{\text{exp}}(\xi) = [Z \quad Q] \exp \left(\begin{bmatrix} -Z^\top \xi & -R^\top \\ R & 0 \end{bmatrix} \right) \begin{bmatrix} I_k \\ 0 \end{bmatrix}.$$

where $QR = -(I_k - ZZ^\top)\xi$ is the unique QR factorization.

- **Polar decomposition.** It takes $3dk^2 + O(k^3)$ flops and has the closed-form expression:

$$\text{Retr}_Z^{\text{polar}}(\xi) = (Z + \xi)(I_k + \xi^\top \xi)^{-1/2}.$$

- **QR decomposition.** It takes $2dk^2 + O(k^3)$ flops and has the closed-form expression:

$$\text{Retr}_Z^{\text{qr}}(\xi) = \text{qr}(Z + \xi),$$

where $\text{qr}(A)$ is the Q factor of the QR factorization of A .

- **Cayley transformation.** It takes $7dk^2 + O(k^3)$ flops and has the closed-form expression:

$$\text{Retr}_Z^{\text{cayley}}(\xi) = \left(I_n - \frac{1}{2}W(\xi) \right)^{-1} \left(I_n + \frac{1}{2}W(\xi) \right) Z,$$

where $W(\xi) = (I_n - ZZ^\top/2)\xi Z^\top - Z\xi^\top(I_n - ZZ^\top/2)$.

We now present a novel approach to exploiting the structure of f . We begin with several definitions.

Definition 2.4 The coefficient matrix between $\mu = \sum_{i=1}^n r_i \delta_{x_i}$ and $\nu = \sum_{j=1}^n c_j \delta_{y_j}$ is defined by $C = (C_{ij})_{1 \leq i, j \leq n} \in \mathbb{R}^{n \times n}$ with each entry $C_{ij} = \|x_i - y_j\|^2$.

Definition 2.5 The correlation matrix between $\mu = \sum_{i=1}^n r_i \delta_{x_i}$ and $\nu = \sum_{j=1}^n c_j \delta_{y_j}$ is defined by $V_\pi = \sum_{i=1}^n \sum_{j=1}^n \pi_{i,j} (x_i - y_j)(x_i - y_j)^\top \in \mathbb{R}^{d \times d}$.

Algorithm 2 Riemannian Adaptive Gradient Ascent with Sinkhorn Iteration (RAGAS)

- 1: **Input:** $\{(x_i, r_i)\}_{i \in [n]}$ and $\{(y_j, c_j)\}_{j \in [n]}$, $k = \tilde{O}(1)$, $U_0 \in \text{St}(d, k)$, ϵ and $\alpha \in (0, 1)$.
- 2: **Initialize:** $p_0 = \mathbf{0}_d$, $q_0 = \mathbf{0}_k$, $\hat{p}_0 = \alpha \|C\|_\infty^2 \mathbf{1}_d$, $\hat{q}_0 = \alpha \|C\|_\infty^2 \mathbf{1}_k$, $\hat{\epsilon} \leftarrow \min\{\epsilon, \frac{\epsilon^2 \alpha}{1000 \|C\|_\infty}\}$, $\eta \leftarrow \frac{\hat{\epsilon}}{4 \log(n)}$ and $\gamma \leftarrow \frac{\alpha}{16L_1^2 + 32L_2 + 32\eta^{-1}L_1^2\|C\|_\infty}$.
- 3: **for** $t = 0, 1, 2, \dots$ **do**
- 4: Compute $\pi_{t+1} \leftarrow \text{REGOT}(\{(x_i, r_i)\}_{i \in [n]}, \{(y_j, c_j)\}_{j \in [n]}, U_t, \eta, \hat{\epsilon})$.
- 5: Compute $G_{t+1} \leftarrow P_{\text{St}}(2V_{\pi_{t+1}}U_t)$.
- 6: Update $p_{t+1} \leftarrow \beta p_t + (1 - \beta) \text{diag}(G_{t+1}G_{t+1}^\top)/k$ and $\hat{p}_{t+1} \leftarrow \max\{\hat{p}_t, p_{t+1}\}$.
- 7: Update $q_{t+1} \leftarrow \beta q_t + (1 - \beta) \text{diag}(G_{t+1}^\top G_{t+1})/d$ and $\hat{q}_{t+1} \leftarrow \max\{\hat{q}_t, q_{t+1}\}$.
- 8: Compute $\xi_{t+1} \leftarrow P_{\text{St}}(\text{Diag}(\hat{p}_{t+1})^{-1/4}G_{t+1}\text{Diag}(\hat{q}_{t+1})^{-1/4})$.
- 9: Compute $U_{t+1} \leftarrow \text{Retr}_{U_t}(\gamma \xi_{t+1})$.
- 10: **end for**

The first lemma shows that the structure of the function f is very bad regardless of nonconvexity and the lack of smoothness.

Lemma 2.2 *The function f is $2\|C\|_\infty$ -weakly concave.*

Proof. By [Vial \[1983, Proposition 4.3\]](#), it suffices to show that the function $f(U) - \|C\|_\infty\|U\|_F^2$ is concave for any $U \in \mathbb{R}^{d \times k}$. By the definition of f , we have

$$f(U) = \min_{\pi \in \Pi(\mu, \nu)} \text{Trace}(U^\top V_\pi U).$$

Since $\{x_1, x_2, \dots, x_n\} \subseteq \mathbb{R}^d$ and $\{y_1, y_2, \dots, y_n\} \subseteq \mathbb{R}^d$ are two given groups of n atoms in \mathbb{R}^d , the coefficient matrix C is independent of U and π . Furthermore, $\sum_{i=1}^n \sum_{j=1}^n \pi_{i,j} = 1$ and $\pi_{i,j} \geq 0$ for all $i, j \in [n]$ since $\pi \in \Pi(\mu, \nu)$. Putting these pieces together with Jensen's inequality, we have

$$\|V_\pi\|_F \leq \sum_{i=1}^n \sum_{j=1}^n \pi_{i,j} \|(x_i - y_j)(x_i - y_j)^\top\|_F \leq \max_{1 \leq i, j \leq n} \|x_i - y_j\|^2 = \|C\|_\infty.$$

This implies that $U \mapsto \text{Trace}(U^\top V_\pi U) - \|C\|_\infty\|U\|_F^2$ is concave for any $\pi \in \Pi(\mu, \nu)$. Since $\Pi(\mu, \nu)$ is compact, Danskin's theorem [\[Rockafellar, 2015\]](#) implies the desired result. \square

The second lemma shows that the subdifferential of the function f is independent of U and bounded by a constant $2\|C\|_\infty$.

Lemma 2.3 *Each element of the subdifferential $\partial f(U)$ is bounded by $2\|C\|_\infty$ for all $U \in \text{St}(d, k)$.*

Proof. By the definition of the subdifferential ∂f , it suffices to show that $\|V_\pi U\|_F \leq \|C\|_\infty$ for all $\pi \in \Pi(\mu, \nu)$ and $U \in \text{St}(d, k)$. Indeed, by the definition, V_π is symmetric and positive semi-definite. Therefore, we have

$$\max_{U \in \text{St}(d, k)} \|V_\pi U\|_F \leq \|V_\pi\|_F \leq \|C\|_\infty.$$

Putting these pieces together yields the desired result. \square

Remark 2.4 Lemma 2.2 implies there exists a concave function $g : \mathbb{R}^{d \times k} \rightarrow \mathbb{R}$ such that $f(U) = g(U) + \|C\|_\infty \|U\|_F^2$ for any $U \in \mathbb{R}^{d \times k}$. Since g is concave, ∂g is well defined and Vial [1983, Proposition 4.6] implies that $\partial f(U) = \partial g(U) + 2\|C\|_\infty U$ for all $U \in \mathbb{R}^{d \times k}$.

This result together with Vial [1983, Proposition 4.5] and Yang et al. [2014, Theorem 5.1] lead to the Riemannian subdifferential defined by $\text{subdiff } f(U) = P_{\text{Tr}_U \text{St}}(\partial f(U))$ for all $U \in \text{St}(d, k)$.

Definition 2.6 The subspace projection $\widehat{U} \in \text{St}(d, k)$ is called an ϵ -approximate optimal subspace projection of f over $\text{St}(d, k)$ in Eq. (2.4) if it satisfies $\text{dist}(0, \text{subdiff } f(\widehat{U})) \leq \epsilon$.

Definition 2.7 The pair of subspace projection and transportation plan $(\widehat{U}, \widehat{\pi}) \in \text{St}(d, k) \times \Pi(\mu, \nu)$ is an ϵ -approximate pair of optimal subspace projection and optimal transportation plan for the computation of the PRW distance in Eq. (2.1) if the following statements hold true: (i) \widehat{U} is an ϵ -approximate optimal subspace projection of f over $\text{St}(d, k)$ in Eq. (2.4). (ii) $\widehat{\pi}$ is an ϵ -approximate optimal transportation plan for the subspace projection \widehat{U} .

The goal of this paper is to develop a set of algorithms which are guaranteed to converge to a pair of approximate optimal subspace projection and optimal transportation plan, which stand for a stationary point of the max-min optimization model in Eq. (2.1). In the next section, we provide the detailed scheme of our algorithm as well as the finite-time theoretical guarantee.

3 Riemannian (Adaptive) Gradient meets Sinkhorn Iteration

We present the *Riemannian gradient ascent with Sinkhorn* (RGAS) algorithm for solving Eq. (2.5). By the definition of V_π (cf. Definition 2.5), we can rewrite $f_\eta(U) = \min_{\pi \in \Pi(\mu, \nu)} \{\langle UU^\top, V_\pi \rangle - \eta H(\pi)\}$. Fix $U \in \mathbb{R}^{d \times k}$, and define the mapping $\pi \mapsto \langle UU^\top, V_\pi \rangle - \eta H(\pi)$ with respect to ℓ_1 -norm. By the compactness of the transportation polytope $\Pi(\mu, \nu)$, Danskin's theorem [Rockafellar, 2015] implies that f_η is smooth. Moreover, by the symmetry of V_π , we have

$$\nabla f_\eta(U) = 2V_{\pi^*(U)}U \quad \text{for any } U \in \mathbb{R}^{d \times k}, \quad (3.1)$$

where $\pi^*(U) := \text{argmin}_{\pi \in \Pi(\mu, \nu)} \{\langle UU^\top, V_\pi \rangle - \eta H(\pi)\}$. This entropic regularized OT is solved inexactly at each inner loop of the maximization and we use the output $\pi_{t+1} \leftarrow \pi(U_t)$ to obtain an inexact gradient of f_η which permits the Riemannian gradient ascent update; see Algorithm 1.

The remaining issue is to approximately solve an entropic regularized OT efficiently. We leverage Cuturi's approach and obtain $\widehat{\pi}$ -approximate optimal transport plan for $U_t \in \text{St}(d, k)$ using the Sinkhorn iteration. It has been shown in Altschuler et al. [2017], Dvurechensky et al. [2018] that Sinkhorn iteration achieves a finite-time guarantee which is polynomial in n and $1/\widehat{\epsilon}$. As a practical enhancement, we exploit the matrix structure of $\text{grad } f_\eta(U_t)$ via the use of two different adaptive weight vectors, namely \widehat{p}_t and \widehat{q}_t (see Algorithm 2). The scaling direction is better than the Riemannian gradient $\text{grad } f_\eta(U_t)$ in terms of robustness to the stepsize; see the adaptive algorithm in Algorithm 2.

3.1 Technical lemmas

We first show that f_η is continuously differentiable over $\mathbb{R}^{d \times k}$ and the classical gradient inequality holds true over $\text{St}(d, k)$. The derivation is novel and uncovers the structure of the computation of entropic

regularized PRW in Eq. (2.3). Let $g : \mathbb{R}^{d \times k} \times \Pi(\mu, \nu) \rightarrow \mathbb{R}$ be defined by

$$g(U, \pi) := \sum_{i=1}^n \sum_{j=1}^n \pi_{i,j} \|U^\top x_i - U^\top y_j\|^2 - \eta H(\pi).$$

Lemma 3.1 f_η is differentiable over $\mathbb{R}^{d \times k}$ and $\|\nabla f_\eta(U)\|_F \leq 2\|C\|_\infty$ for all $U \in \text{St}(d, k)$.

Proof. It is clear that we have $f_\eta(\bullet) = \min_{\pi \in \Pi(\mu, \nu)} g(\bullet, \pi)$. Furthermore, $\pi^*(\bullet) = \operatorname{argmin}_{\pi \in \Pi(\mu, \nu)} g(\bullet, \pi)$ is uniquely defined. Putting these pieces with the compactness of $\Pi(\mu, \nu)$ and the smoothness of $g(\bullet, \pi)$, Danskin's theorem [Rockafellar, 2015] implies f_η is continuously differentiable and the gradient is

$$\nabla f_\eta(U) = 2V_{\pi^*(U)}U \quad \text{for all } U \in \mathbb{R}^{d \times k}.$$

Since $U \in \text{St}(d, k)$ and $\pi^*(U) \in \Pi(\mu, \nu)$, we have

$$\|\nabla f_\eta(U)\|_F = 2\|V_{\pi^*(U)}U\|_F \leq 2\|V_{\pi^*(U)}\|_F \leq 2\|C\|_\infty.$$

This completes the proof. \square

Lemma 3.2 For all $U_1, U_2 \in \text{St}(d, k)$, the following statement holds true,

$$|f_\eta(U_1) - f_\eta(U_2) - \langle \nabla f_\eta(U_2), U_1 - U_2 \rangle| \leq \left(\|C\|_\infty + \frac{2\|C\|_\infty^2}{\eta} \right) \|U_1 - U_2\|_F^2.$$

Proof. It suffices to prove that

$$\|\nabla f_\eta(\alpha U_1 + (1 - \alpha)U_2) - \nabla f_\eta(U_2)\|_F \leq \left(2\|C\|_\infty + \frac{4\|C\|_\infty^2}{\eta} \right) \alpha \|U_1 - U_2\|_F,$$

for any $U_1, U_2 \in \text{St}(d, k)$ and any $\alpha \in [0, 1]$. Indeed, let $U_\alpha = \alpha U_1 + (1 - \alpha)U_2$, we have

$$\|\nabla f_\eta(U_\alpha) - \nabla f_\eta(U_2)\|_F \leq 2\|V_{\pi^*(U_\alpha)}\|_F \|U_\alpha - U_2\|_F + 2\|V_{\pi^*(U_\alpha)} - V_{\pi^*(U_2)}\|_F.$$

Since $\pi^*(U_\alpha) \in \Pi(\mu, \nu)$, we have $\|V_{\pi^*(U_\alpha)}\|_F \leq \|C\|_\infty$. By the definition of V_π , we have

$$\|V_{\pi^*(U_\alpha)} - V_{\pi^*(U_2)}\|_F \leq \sum_{i=1}^n \sum_{j=1}^n |\pi_{i,j}^*(U_\alpha) - \pi_{i,j}^*(U_2)| \|x_i - y_j\|^2 \leq \|C\|_\infty \|\pi^*(U_\alpha) - \pi^*(U_2)\|_1.$$

Putting these pieces together yields that

$$\|\nabla f_\eta(U_\alpha) - \nabla f_\eta(U_2)\|_F \leq 2\|C\|_\infty \|U_\alpha - U_2\|_F + 2\|C\|_\infty \|\pi^*(U_\alpha) - \pi^*(U_2)\|_1. \quad (3.2)$$

Using the property of the entropy regularization $H(\bullet)$, we have $g(U, \bullet)$ is strongly convex with respect to ℓ_1 -norm and the module is η . This implies that

$$\begin{aligned} g(U_\alpha, \pi^*(U_2)) - g(U_\alpha, \pi^*(U_\alpha)) - \langle \nabla_\pi g(U_\alpha, \pi^*(U_\alpha)), \pi^*(U_2) - \pi^*(U_\alpha) \rangle \\ \geq (\eta/2) \|\pi^*(U_\alpha) - \pi^*(U_2)\|_1^2, \\ g(U_\alpha, \pi^*(U_\alpha)) - g(U_\alpha, \pi^*(U_2)) - \langle \nabla_\pi g(U_\alpha, \pi^*(U_2)), \pi^*(U_\alpha) - \pi^*(U_2) \rangle \\ \geq (\eta/2) \|\pi^*(U_\alpha) - \pi^*(U_2)\|_1^2. \end{aligned}$$

Summing up these inequalities yields

$$\langle \nabla_{\pi} g(U_{\alpha}, \pi^*(U_{\alpha})) - \nabla_{\pi} g(U_{\alpha}, \pi^*(U_2)), \pi^*(U_{\alpha}) - \pi^*(U_2) \rangle \geq \eta \|\pi^*(U_{\alpha}) - \pi^*(U_2)\|_1^2. \quad (3.3)$$

Furthermore, by the first-order optimality condition of $\pi^*(U_1)$ and $\pi^*(U_2)$, we have

$$\begin{aligned} \langle \nabla_{\pi} g(U_{\alpha}, \pi^*(U_{\alpha})), \pi^*(U_2) - \pi^*(U_{\alpha}) \rangle &\geq 0, \\ \langle \nabla_{\pi} g(U_2, \pi^*(U_2)), \pi^*(U_{\alpha}) - \pi^*(U_2) \rangle &\geq 0. \end{aligned}$$

Summing up these inequalities yields

$$\langle \nabla_{\pi} g(U_2, \pi^*(U_2)) - \nabla_{\pi} g(U_{\alpha}, \pi^*(U_{\alpha})), \pi^*(U_{\alpha}) - \pi^*(U_2) \rangle \geq 0. \quad (3.4)$$

Summing up Eq. (3.3) and Eq. (3.4) and further using Hölder's inequality, we have

$$\|\pi^*(U_{\alpha}) - \pi^*(U_2)\|_1 \leq (1/\eta) \|\nabla_{\pi} g(U_2, \pi^*(U_2)) - \nabla_{\pi} g(U_{\alpha}, \pi^*(U_2))\|_{\infty}.$$

By the definition of function g , we have

$$\begin{aligned} \|\nabla_{\pi} g(U_2, \pi^*(U_2)) - \nabla_{\pi} g(U_{\alpha}, \pi^*(U_2))\|_{\infty} &\leq \max_{1 \leq i, j \leq n} |(x_i - x_j)^T (U_2 U_2^T - U_{\alpha} U_{\alpha}^T)(x_i - x_j)| \\ &\leq \left(\max_{1 \leq i, j \leq n} \|x_i - x_j\|^2 \right) \|U_2 U_2^T - U_{\alpha} U_{\alpha}^T\|_F \\ &= \|C\|_{\infty} \|U_2 U_2^T - U_{\alpha} U_{\alpha}^T\|_F. \end{aligned}$$

Since $U_1, U_2 \in \text{St}(d, k)$, we have

$$\begin{aligned} \|U_2 U_2^T - U_{\alpha} U_{\alpha}^T\|_F &\leq \|U_2 (U_2 - U_{\alpha})^T\|_F + \|(U_2 - U_{\alpha}) U_{\alpha}^T\|_F \\ &\leq \|U_2 - U_{\alpha}\|_F + \|(U_2 - U_{\alpha})(\alpha U_1 + (1 - \alpha) U_2)^T\|_F \\ &\leq \|U_2 - U_{\alpha}\|_F + \alpha \|(U_2 - U_{\alpha}) U_1^T\|_F + (1 - \alpha) \|(U_2 - U_{\alpha}) U_2^T\|_F \\ &\leq 2 \|U_2 - U_{\alpha}\|_F. \end{aligned}$$

Putting these pieces together yields that

$$\|\pi^*(U_{\alpha}) - \pi^*(U_2)\|_1 \leq \frac{2\|C\|_{\infty}}{\eta} \|U_{\alpha} - U_2\|_F. \quad (3.5)$$

Plugging Eq. (3.5) into Eq. (3.2) yields the desired result. \square

Remark 3.3 Lemma 3.2 shows that f_{η} satisfies the classical gradient inequality over the Stiefel manifold. This is indeed stronger than the following statement,

$$\|\nabla f_{\eta}(U_1) - \nabla f_{\eta}(U_2)\|_F \leq \left(2\|C\|_{\infty} + \frac{4\|C\|_{\infty}^2}{\eta} \right) \|U_1 - U_2\|_F, \quad \text{for all } U_1, U_2 \in \text{St}(d, k),$$

and forms the basis for analyzing the complexity bound of Algorithm 1 and 2. The techniques used in proving Lemma 3.2 are new and may be applicable to analyze the structure of the robust variant of the Wasserstein distance with other type of regularization [Dessein et al., 2018, Blondel et al., 2018].

Then we quantify the progress of RGAS algorithm (cf. Algorithm 1) using f_η as a potential function and then provide an upper bound for the number of iterations to return an ϵ -approximate optimal subspace projection $U_t \in \text{St}(d, k)$ satisfying $\text{dist}(0, \text{subdiff } f(U_t)) \leq \epsilon$ in Algorithm 1.

Lemma 3.4 *Let $\{(U_t, \pi_t)\}_{t \geq 1}$ be the iterates generated by Algorithm 1. We have*

$$\frac{1}{T} \left(\sum_{t=0}^{T-1} \|\text{grad } f_\eta(U_t)\|_F^2 \right) \leq \frac{4\Delta_f}{\gamma T} + \frac{\epsilon^2}{5},$$

where $\Delta_f = \max_{U \in \text{St}(d, k)} f_\eta(U) - f_\eta(U_0)$ is the initial objective gap.

Proof. Using Lemma 3.2 with $U_1 = U_{t+1}$ and $U_2 = U_t$, we have

$$f_\eta(U_{t+1}) - f_\eta(U_t) - \langle \nabla f_\eta(U_t), U_{t+1} - U_t \rangle \geq - \left(\|C\|_\infty + \frac{2\|C\|_\infty^2}{\eta} \right) \|U_{t+1} - U_t\|_F^2. \quad (3.6)$$

By the definition of U_{t+1} , we have

$$\begin{aligned} \langle \nabla f_\eta(U_t), U_{t+1} - U_t \rangle &= \langle \nabla f_\eta(U_t), \text{Retr}_{U_t}(\gamma \xi_{t+1}) - U_t \rangle \\ &= \langle \nabla f_\eta(U_t), \gamma \xi_{t+1} \rangle + \langle \nabla f_\eta(U_t), \text{Retr}_{U_t}(\gamma \xi_{t+1}) - (U_t + \gamma \xi_{t+1}) \rangle \\ &\geq \langle \nabla f_\eta(U_t), \gamma \xi_{t+1} \rangle - \|\nabla f_\eta(U_t)\|_F \|\text{Retr}_{U_t}(\gamma \xi_{t+1}) - (U_t + \gamma \xi_{t+1})\|_F. \end{aligned}$$

By Lemma 3.1, we have $\|\nabla f_\eta(U)\|_F \leq 2\|C\|_\infty$. Putting these pieces with Proposition 2.1 yields that

$$\langle \nabla f_\eta(U_t), U_{t+1} - U_t \rangle \geq \gamma \langle \nabla f_\eta(U_t), \xi_{t+1} \rangle - 2\gamma^2 L_2 \|C\|_\infty \|\xi_{t+1}\|_F^2. \quad (3.7)$$

Using Proposition 2.1 again, we have

$$\|U_{t+1} - U_t\|_F^2 = \|\text{Retr}_{U_t}(\gamma \xi_{t+1}) - U_t\|_F^2 \leq \gamma^2 L_1^2 \|\xi_{t+1}\|_F^2. \quad (3.8)$$

Combining Eq. (3.6), Eq. (3.7) and Eq. (3.8) yields

$$f_\eta(U_{t+1}) - f_\eta(U_t) \geq \gamma \langle \nabla f_\eta(U_t), \xi_{t+1} \rangle - \gamma^2 ((L_1^2 + 2L_2) \|C\|_\infty + 2\eta^{-1} L_1^2 \|C\|_\infty^2) \|\xi_{t+1}\|_F^2. \quad (3.9)$$

Recall that $\text{grad } f_\eta(U_t) = P_{\text{T}_{U_t} \text{St}}(\nabla f_\eta(U_t))$ and $\xi_{t+1} = P_{\text{T}_{U_t} \text{St}}(2V_{\pi_{t+1}} U_t)$, we have

$$\langle \nabla f_\eta(U_t), \xi_{t+1} \rangle = \langle \text{grad } f_\eta(U_t), \xi_{t+1} \rangle = \|\text{grad } f_\eta(U_t)\|_F^2 + \langle \text{grad } f_\eta(U_t), \xi_{t+1} - \text{grad } f_\eta(U_t) \rangle$$

Using Young's inequality, we have

$$\langle \nabla f_\eta(U_t), \xi_{t+1} \rangle \geq (1/2) (\|\text{grad } f_\eta(U_t)\|_F^2 - \|\xi_{t+1} - \text{grad } f_\eta(U_t)\|_F^2).$$

Furthermore, we have $\|\xi_{t+1}\|_F^2 \leq 2\|\text{grad } f_\eta(U_t)\|_F^2 + 2\|\xi_{t+1} - \text{grad } f_\eta(U_t)\|_F^2$. Putting these pieces together with Eq. (3.9) yields that

$$\begin{aligned} f_\eta(U_{t+1}) - f_\eta(U_t) &\geq \gamma \left(\frac{1}{2} - \gamma (2L_1^2 \|C\|_\infty + 4L_2 \|C\|_\infty + 4\eta^{-1} L_1^2 \|C\|_\infty^2) \right) \|\text{grad } f_\eta(U_t)\|_F^2 \\ &\quad - \gamma \left(\frac{1}{2} + \gamma (2L_1^2 \|C\|_\infty + 4L_2 \|C\|_\infty + 4\eta^{-1} L_1^2 \|C\|_\infty^2) \right) \|\xi_{t+1} - \text{grad } f_\eta(U_t)\|_F^2. \end{aligned} \quad (3.10)$$

Since $\xi_{t+1} = P_{\text{Tr}_{U_t} \text{St}}(2V_{\pi_{t+1}}U_t)$ and $\text{grad } f_\eta(U_t) = P_{\text{Tr}_{U_t} \text{St}}(2V_{\tilde{\pi}_t^*}U_t)$ where $\tilde{\pi}_t^*$ is a minimizer of the entropic regularized OT problem, i.e., $\tilde{\pi}_t^* \in \text{argmin}_{\pi \in \Pi(\mu, \nu)} \{ \langle U_t U_t^\top, V_\pi \rangle - \eta H(\pi) \}$, we have

$$\|\xi_{t+1} - \text{grad } f_\eta(U_t)\|_F^2 \leq 4\|(V_{\pi_{t+1}} - V_{\tilde{\pi}_t^*})U_t\|_F^2.$$

Furthermore, by letting π_t^* be a minimizer of the unregularized OT problem with U_t , i.e., $\pi_t^* \in \text{argmin}_{\pi \in \Pi(\mu, \nu)} \langle U_t U_t^\top, V_\pi \rangle$, we have

$$\|(V_{\pi_{t+1}} - V_{\tilde{\pi}_t^*})U_t\|_F^2 \leq 2\|(V_{\pi_{t+1}} - V_{\pi_t^*})U_t\|_F^2 + 2\|(V_{\tilde{\pi}_t^*} - V_{\pi_t^*})U_t\|_F^2.$$

Collecting these bounds leads to the following inequality

$$\|\xi_{t+1} - \text{grad } f_\eta(U_t)\|_F^2 \leq 8\|(V_{\pi_{t+1}} - V_{\pi_t^*})U_t\|_F^2 + 8\|(V_{\tilde{\pi}_t^*} - V_{\pi_t^*})U_t\|_F^2.$$

By the definition of the subroutine $\text{REGOT}(\{(x_i, r_i)\}_{i \in [n]}, \{(y_j, c_j)\}_{j \in [n]}, U, \hat{\epsilon})$, we have

$$\pi_{t+1} \in \Pi(\mu, \nu), \quad 0 \leq \langle U_t U_t^\top, V_{\pi_{t+1}} - V_{\pi_t^*} \rangle \leq \hat{\epsilon}.$$

By the definition of $\tilde{\pi}_t^*$, we have $\langle U_t U_t^\top, V_{\tilde{\pi}_t^*} \rangle - \eta H(\tilde{\pi}_t^*) \leq \langle U_t U_t^\top, V_{\pi_t^*} \rangle - \eta H(\pi_t^*)$. Since $0 \leq H(\pi) - 1 \leq 2 \log(n)$ and $\eta = \hat{\epsilon}/(4 \log(n))$, we have

$$0 \leq \langle U_t U_t^\top, V_{\tilde{\pi}_t^*} - V_{\pi_t^*} \rangle \leq \hat{\epsilon}/2. \quad (3.11)$$

This together with $\|V_{\pi_{t+1}} - V_{\pi_t^*}\|_F \leq 2\|C\|_\infty$ and $\|V_{\tilde{\pi}_t^*} - V_{\pi_t^*}\|_F \leq 2\|C\|_\infty$ yields

$$\|\xi_{t+1} - \text{grad } f_\eta(U_t)\|_F^2 \leq 16\|C\|_\infty \hat{\epsilon}. \quad (3.12)$$

Plugging Eq. (3.12) into Eq. (3.10) with the definition of γ and $\hat{\epsilon} \leq \epsilon^2/(500\|C\|_\infty)$ yields that

$$f_\eta(U_{t+1}) - f_\eta(U_t) \geq \frac{\gamma \|\text{grad } f_\eta(U_t)\|_F^2}{4} - \frac{\gamma \epsilon^2}{20}.$$

Summing and rearranging the resulting inequality yields that

$$\frac{1}{T} \left(\sum_{t=0}^{T-1} \|\text{grad } f_\eta(U_t)\|_F^2 \right) \leq \frac{4(f_\eta(U_T) - f_\eta(U_0))}{\gamma T} + \frac{\epsilon^2}{5}.$$

This together with the definition of Δ_f implies the desired result. \square

We now provide analogous results for the RAGAS algorithm (cf. Algorithm 2).

Lemma 3.5 *Let $\{(U_t, \pi_t)\}_{t \geq 1}$ be the iterates generated by Algorithm 2. Then, we have*

$$\frac{1}{T} \left(\sum_{t=0}^{T-1} \|\text{grad } f_\eta(U_t)\|_F^2 \right) \leq \frac{8\|C\|_\infty \Delta_f}{\gamma T} + \frac{\epsilon^2}{3},$$

where $\Delta_f = \max_{U \in \text{St}(d, k)} f_\eta(U) - f_\eta(U_0)$ is the initial objective gap.

Proof. Using the same argument as in the proof of Lemma 3.4, we have

$$f_\eta(U_{t+1}) - f_\eta(U_t) \geq \gamma \langle \nabla f_\eta(U_t), \xi_{t+1} \rangle - \gamma^2 ((L_1^2 + 2L_2) \|C\|_\infty + 2\eta^{-1} L_1^2 \|C\|_\infty^2) \|\xi_{t+1}\|_F^2. \quad (3.13)$$

Recall that $\text{grad } f_\eta(U_t) = P_{\text{T}_{U_t}\text{St}}(\nabla f_\eta(U_t))$ and the definition of ξ_{t+1} , we have

$$\begin{aligned} \langle \nabla f_\eta(U_t), \xi_{t+1} \rangle &= \langle \text{grad } f_\eta(U_t), \xi_{t+1} \rangle \\ &= \langle \text{grad } f_\eta(U_t), \text{Diag}(\hat{p}_{t+1})^{-1/4} (\text{grad } f_\eta(U_t)) \text{Diag}(\hat{q}_{t+1})^{-1/4} \rangle \\ &\quad + \langle \text{grad } f_\eta(U_t), \text{Diag}(\hat{p}_{t+1})^{-1/4} (G_{t+1} - \text{grad } f_\eta(U_t)) \text{Diag}(\hat{q}_{t+1})^{-1/4} \rangle. \end{aligned}$$

Using the Cauchy-Schwarz inequality and the nonexpansiveness of $P_{\text{T}_{U_t}\text{St}}$, we have

$$\begin{aligned} \|\xi_{t+1}\|_F^2 &\leq 2\|P_{\text{T}_{U_t}\text{St}}(\text{Diag}(\hat{p}_{t+1})^{-1/4} (\text{grad } f_\eta(U_t)) \text{Diag}(\hat{q}_{t+1})^{-1/4})\|_F^2 \\ &\quad + 2\|\xi_{t+1} - P_{\text{T}_{U_t}\text{St}}(\text{Diag}(\hat{p}_{t+1})^{-1/4} (\text{grad } f_\eta(U_t)) \text{Diag}(\hat{q}_{t+1})^{-1/4})\|_F^2 \\ &\leq 2\|\text{Diag}(\hat{p}_{t+1})^{-1/4} (\text{grad } f_\eta(U_t)) \text{Diag}(\hat{q}_{t+1})^{-1/4}\|_F^2 \\ &\quad + 2\|\text{Diag}(\hat{p}_{t+1})^{-1/4} (G_{t+1} - \text{grad } f_\eta(U_t)) \text{Diag}(\hat{q}_{t+1})^{-1/4}\|_F^2. \end{aligned}$$

Furthermore, by the definition of G_{t+1} , we have $\|G_{t+1}\|_F \leq 2\|C\|_\infty$ and hence

$$\mathbf{0}_d \leq \frac{\text{diag}(G_{t+1} G_{t+1}^\top)}{k} \leq 4\|C\|_\infty^2 \mathbf{1}_d, \quad \mathbf{0}_k \leq \frac{\text{diag}(G_{t+1}^\top G_{t+1})}{d} \leq 4\|C\|_\infty^2 \mathbf{1}_k.$$

By the definition of p_t and q_t , we have $\mathbf{0}_d \preceq p_t \preceq 4\|C\|_\infty^2 \mathbf{1}_d$ and $\mathbf{0}_k \preceq q_t \preceq 4\|C\|_\infty^2 \mathbf{1}_k$. This together with the definition of \hat{p}_t and \hat{q}_t implies that

$$\alpha\|C\|_\infty^2 \mathbf{1}_d \leq \hat{p}_t \leq 4\|C\|_\infty^2 \mathbf{1}_d, \quad \alpha\|C\|_\infty^2 \mathbf{1}_k \leq \hat{q}_t \leq 4\|C\|_\infty^2 \mathbf{1}_k.$$

This inequality together with Young's inequality implies that

$$\begin{aligned} \langle \nabla f_\eta(U_t), \xi_{t+1} \rangle &\geq \frac{\|\text{grad } f_\eta(U_t)\|_F^2}{2\|C\|_\infty} - \frac{1}{\sqrt{\alpha}\|C\|_\infty} \left(\frac{\sqrt{\alpha}\|\text{grad } f_\eta(U_t)\|_F^2}{4} + \frac{\|G_{t+1} - \text{grad } f_\eta(U_t)\|_F^2}{\sqrt{\alpha}} \right) \\ &= \frac{\|\text{grad } f_\eta(U_t)\|_F^2}{4\|C\|_\infty} - \frac{\|G_{t+1} - \text{grad } f_\eta(U_t)\|_F^2}{\alpha\|C\|_\infty}, \end{aligned}$$

and

$$\|\xi_{t+1}\|_F^2 \leq \frac{2\|\text{grad } f_\eta(U_t)\|_F^2}{\alpha\|C\|_\infty^2} + \frac{2\|G_{t+1} - \text{grad } f_\eta(U_t)\|_F^2}{\alpha\|C\|_\infty^2}.$$

Putting these pieces together with Eq. (3.13) yields that

$$\begin{aligned} f_\eta(U_{t+1}) - f_\eta(U_t) &\geq \frac{\gamma}{4\|C\|_\infty} \left(1 - \frac{8\gamma}{\alpha} (L_1^2 + 2L_2 + 2\eta^{-1} L_1^2 \|C\|_\infty) \right) \|\text{grad } f_\eta(U_t)\|_F^2 \\ &\quad - \frac{\gamma}{\alpha\|C\|_\infty} (1 + \gamma(2L_1^2 + 4L_2 + 4\eta^{-1} L_1^2 \|C\|_\infty)) \|G_{t+1} - \text{grad } f_\eta(U_t)\|_F^2. \end{aligned} \quad (3.14)$$

Recall that $G_{t+1} = P_{\text{T}_{U_t}\text{St}}(2V_{\pi_{t+1}} U_t)$ and $\text{grad } f_\eta(U_t) = P_{\text{T}_{U_t}\text{St}}(2V_{\tilde{\pi}_t^*} U_t)$. Then we can apply the same argument as in the proof of Lemma 3.4 and obtain that

$$\|G_{t+1} - \text{grad } f_\eta(U_t)\|_F^2 \leq 16\|C\|_\infty \hat{\epsilon}. \quad (3.15)$$

Plugging Eq. (3.15) into Eq. (3.14) with the definition of γ and $\hat{\epsilon} \leq \epsilon^2 \alpha / (1000 \|C\|_\infty)$ yields that

$$f_\eta(U_{t+1}) - f_\eta(U_t) \geq \frac{\gamma \|\text{grad } f_\eta(U_t)\|_F^2}{8\|C\|_\infty} - \frac{\gamma \epsilon^2}{30}.$$

Summing and rearranging the resulting inequality yields that

$$\frac{1}{T} \left(\sum_{t=0}^{T-1} \|\text{grad } f_\eta(U_t)\|_F^2 \right) \leq \frac{8\|C\|_\infty (f_\eta(U_T) - f_\eta(U_0))}{\gamma T} + \frac{\epsilon^2}{3}.$$

This together with the definition of Δ_f implies the desired result. \square

3.2 Main results

We present the iteration complexity of the RGAS algorithm (Algorithm 1) and the RAGAS algorithm (Algorithm 2) in the following two theorems.

Theorem 3.6 *Letting $\{(U_t, \pi_t)\}_{t \geq 1}$ be the iterates generated by Algorithm 1, the number of iterations required to reach $\text{dist}(0, \text{subdiff } f(U_t)) \leq \epsilon$ satisfies that*

$$t = \tilde{O} \left(\frac{k\|C\|_\infty^2}{\epsilon^2} \left(1 + \max \left\{ \frac{\|C\|_\infty}{\epsilon}, \frac{\|C\|_\infty^2}{\epsilon^2} \right\} \right)^2 \right).$$

Proof. Recall that $\tilde{\pi}_t^*$ and π_t^* are defined as the minimizers of entropy-regularized OT problem and unregularized OT problem, i.e.,

$$\tilde{\pi}_t^* \in \underset{\pi \in \Pi(\mu, \nu)}{\text{argmin}} \langle U_t U_t^\top, V_\pi \rangle - \eta H(\pi), \quad \pi_t^* \in \underset{\pi \in \Pi(\mu, \nu)}{\text{argmin}} \langle U_t U_t^\top, V_\pi \rangle.$$

This implies that $\nabla f_\eta(U_t) = 2V_{\tilde{\pi}_t^*}U_t$ and $2V_{\pi_t^*}U_t \in \partial f(U_t)$. By the definition of Riemannian gradient and Riemannian subdifferential, we have

$$\begin{aligned} \text{grad } f_\eta(U_t) &= P_{\text{T}_{U_t}\text{St}}(2V_{\tilde{\pi}_t^*}U_t), \\ \text{subdiff } f(U_t) &\ni P_{\text{T}_{U_t}\text{St}}(2V_{\pi_t^*}U_t). \end{aligned}$$

Therefore, we conclude that

$$\begin{aligned} \text{dist}(0, \text{subdiff } f(U_t)) &\leq \|P_{\text{T}_{U_t}\text{St}}(2V_{\pi_t^*}U_t)\|_F \\ &\leq \|P_{\text{T}_{U_t}\text{St}}(2V_{\tilde{\pi}_t^*}U_t)\|_F + \|P_{\text{T}_{U_t}\text{St}}(2V_{\pi_t^*}U_t) - P_{\text{T}_{U_t}\text{St}}(2V_{\tilde{\pi}_t^*}U_t)\|_F \\ &\leq \|\text{grad } f_\eta(U_t)\|_F + 2\|(V_{\pi_t^*} - V_{\tilde{\pi}_t^*})U_t\|_F. \end{aligned}$$

Since $\pi_t^*, \tilde{\pi}_t^* \in \Pi(\mu, \nu)$, we have $\|V_{\tilde{\pi}_t^*} - V_{\pi_t^*}\|_F \leq 2\|C\|_\infty$. Combining this with Eq. (3.11) yields that

$$\|(V_{\pi_t^*} - V_{\tilde{\pi}_t^*})U_t\|_F^2 \leq \|C\|_\infty \hat{\epsilon} \leq \frac{\epsilon^2}{500}.$$

Putting these pieces together yields

$$\text{dist}(0, \text{subdiff } f(U_t)) \leq \|\text{grad } f_\eta(U_t)\|_F + \frac{\epsilon}{10}.$$

Combining this inequality with Lemma 3.4 and the Cauchy-Schwarz inequality, we have

$$\begin{aligned} \frac{1}{T} \left(\sum_{t=0}^{T-1} [\text{dist}(0, \text{subdiff } f(U_t))]^2 \right) &\leq \frac{2}{T} \left(\sum_{t=0}^{T-1} \|\text{grad } f_\eta(U_t)\|_F^2 \right) + \frac{\epsilon^2}{50} \leq \frac{8\Delta_f}{\gamma T} + \frac{2\epsilon^2}{5} + \frac{\epsilon^2}{50} \\ &\leq \frac{8\Delta_f}{\gamma T} + \frac{\epsilon^2}{2}. \end{aligned}$$

Given that $\text{dist}(0, \text{subdiff } f(U_t)) > \epsilon$ for all $t = 0, 1, \dots, T-1$ and

$$\begin{aligned} \frac{1}{\gamma} &= (8L_1^2 + 16L_2)\|C\|_\infty + \frac{16L_1^2\|C\|_\infty^2}{\eta} = (8L_1^2 + 16L_2)\|C\|_\infty + \frac{64L_1^2\|C\|_\infty^2 \log(n)}{\hat{\epsilon}} \\ &= (8L_1^2 + 16L_2)\|C\|_\infty + 64L_1^2\|C\|_\infty^2 \log(n) \max \left\{ \frac{1}{\epsilon}, \frac{500\|C\|_\infty}{\epsilon^2} \right\}, \end{aligned}$$

we conclude that the upper bound T must satisfy

$$\epsilon^2 \leq \frac{16\Delta_f}{T} \left((8L_1^2 + 16L_2)\|C\|_\infty + 64L_1^2\|C\|_\infty^2 \log(n) \max \left\{ \frac{\|C\|_\infty}{\epsilon}, \frac{500\|C\|_\infty^2}{\epsilon^2} \right\} \right).$$

Using Lemma 3.2, we have

$$\begin{aligned} \Delta_f &\leq \left(\|C\|_\infty + \frac{2\|C\|_\infty^2}{\eta} \right) \left(\max_{U \in \text{St}(d, k)} \|U - U_0\|_F^2 \right) = k \left(2\|C\|_\infty + \frac{4\|C\|_\infty^2}{\eta} \right) \\ &= k \left(2\|C\|_\infty + 16\|C\|_\infty \log(n) \max \left\{ \frac{\|C\|_\infty}{\epsilon}, \frac{500\|C\|_\infty^2}{\epsilon^2} \right\} \right). \end{aligned}$$

Putting these pieces together implies the desired result. \square

Theorem 3.7 *Letting $\{(U_t, \pi_t)\}_{t \geq 1}$ be the iterates generated by Algorithm 2, the number of iterations required to reach $\text{dist}(0, \text{subdiff } f(U_t)) \leq \epsilon$ satisfies*

$$t = \tilde{O} \left(\frac{k\|C\|_\infty^2}{\epsilon^2} \left(1 + \max \left\{ \frac{\|C\|_\infty}{\epsilon}, \frac{\|C\|_\infty^2}{\epsilon^2} \right\} \right)^2 \right).$$

Proof. Using the same argument as in the proof of Theorem 3.6, we have

$$\text{dist}(0, \text{subdiff } f(U_t)) \leq \|\text{grad } f_\eta(U_t)\|_F + \frac{\epsilon}{10}.$$

Combining this inequality with Lemma 3.5 and the Cauchy-Schwarz inequality, we have

$$\begin{aligned} \frac{1}{T} \left(\sum_{t=0}^{T-1} [\text{dist}(0, \text{subdiff } f(U_t))]^2 \right) &\leq \frac{2}{T} \left(\sum_{t=0}^{T-1} \|\text{grad } f_\eta(U_t)\|_F^2 \right) + \frac{\epsilon^2}{50} \\ &\leq \frac{16\|C\|_\infty \Delta_f}{\gamma T} + \frac{2\epsilon^2}{3} + \frac{\epsilon^2}{50} \leq \frac{16\|C\|_\infty \Delta_f}{\gamma T} + \frac{3\epsilon^2}{4}. \end{aligned}$$

Given that $\text{dist}(0, \text{subdiff } f(U_t)) > \epsilon$ for all $t = 0, 1, \dots, T-1$ and

$$\frac{1}{\gamma} = 16L_1^2 + 32L_2 + 128L_1^2\|C\|_\infty \log(n) \max \left\{ \frac{1}{\epsilon}, \frac{1000\|C\|_\infty}{\epsilon^2 \alpha} \right\},$$

we conclude that the upper bound T must satisfies

$$\epsilon^2 \leq \frac{64\|C\|_\infty \Delta_f}{T} \left(16L_1^2 + 32L_2 + 128L_1^2 \log(n) \max \left\{ \frac{\|C\|_\infty}{\epsilon}, \frac{1000\|C\|_\infty^2}{\epsilon^2 \alpha} \right\} \right).$$

Using Lemma 3.2, we have

$$\begin{aligned} \Delta_f &\leq \left(\|C\|_\infty + \frac{2\|C\|_\infty^2}{\eta} \right) \left(\max_{U \in \text{St}(d,k)} \|U - U_0\|_F^2 \right) = k \left(2\|C\|_\infty + \frac{4\|C\|_\infty^2}{\eta} \right) \\ &= k \left(2\|C\|_\infty + 16\|C\|_\infty \log(n) \max \left\{ \frac{\|C\|_\infty}{\epsilon}, \frac{1000\|C\|_\infty^2}{\epsilon^2 \alpha} \right\} \right) \end{aligned}$$

Putting these pieces together implies the desired result. \square

From Theorem 3.6 and 3.7, Algorithm 1 and 2 achieve the same iteration complexity. Furthermore, the number of arithmetic operations at each loop of Algorithm 1 and 2 are also the same. Thus, the complexity bound of Algorithm 2 is the same as that of Algorithm 1.

Theorem 3.8 *Either the RGAS algorithm or the RAGAS algorithm returns an ϵ -approximate pair of optimal subspace projection and optimal transportation plan of the computation of the PRW distance in Eq. (2.1) (cf. Definition 2.7) in*

$$\tilde{O} \left(\left(\frac{n^2 d \|C\|_\infty^2}{\epsilon^2} + \frac{n^2 \|C\|_\infty^4}{\epsilon^4} \max \left\{ 1, \frac{\|C\|_\infty^2}{\epsilon^2} \right\} \right) \left(1 + \max \left\{ \frac{\|C\|_\infty}{\epsilon}, \frac{\|C\|_\infty^2}{\epsilon^2} \right\} \right)^2 \right)$$

arithmetic operations.

Proof. First, Theorem 3.6 implies that the iteration complexity of Algorithm 1 is

$$t = \tilde{O} \left(\frac{k\|C\|_\infty^2}{\epsilon^2} \left(1 + \max \left\{ \frac{\|C\|_\infty}{\epsilon}, \frac{\|C\|_\infty^2}{\epsilon^2} \right\} \right)^2 \right). \quad (3.16)$$

This implies that U_t is an ϵ -approximate optimal subspace projection of problem (2.4). By the definition of $\hat{\epsilon}$ and the subroutine REGOT($\{(x_i, r_i)\}_{i \in [n]}, \{(y_j, c_j)\}_{j \in [n]}, U_t, \eta, \hat{\epsilon}$), we have $\pi_{t+1} \in \Pi(\mu, \nu)$ and

$$0 \leq \langle U_t U_t^\top, V_{\pi_{t+1}} - V_{\pi_t^*} \rangle \leq \hat{\epsilon} \leq \epsilon.$$

This implies that π_{t+1} is an ϵ -approximate optimal transportation plan for the subspace projection U_t . Therefore, we conclude that $(U_t, \pi_{t+1}) \in \text{St}(d, k) \times \Pi(\mu, \nu)$ is an ϵ -approximate pair of optimal subspace projection and optimal transportation plan of problem (2.1). The remaining step is to analyze the complexity bound. Using existing results from Dvurechensky et al. [2018], Lin et al. [2019a] and the definition of $\hat{\epsilon}$, the number of arithmetic operations required by the Sinkhorn iteration or greedy Sinkhorn iteration at each loop is upper bounded by

$$\tilde{O} \left(\frac{n^2 \|C\|_\infty^2}{\epsilon^2} \max \left\{ 1, \frac{\|C\|_\infty^2}{\epsilon^2} \right\} \right).$$

Furthermore, while **Step 5** and **Step 6** in Algorithm 1 can be implemented in $O(dk^2 + k^3)$ arithmetic operations, we still need to construct $V_{\pi_{t+1}} U_t$. A naive approach suggests to first construct $V_{\pi_{t+1}}$ using

$O(n^2dk)$ arithmetic operations and then perform the matrix multiplication using $O(d^2k)$ arithmetic operations. This is computationally prohibitive since d can be very large in practice. In contrast, we observe that

$$V_{\pi_{t+1}} U_t = \sum_{i=1}^n \sum_{j=1}^n (\pi_{t+1})_{i,j} (x_i - y_j) (x_i - y_j)^\top U_t.$$

Since $x_i - y_j \in \mathbb{R}^d$, it will take $O(dk)$ arithmetic operations for computing $(x_i - y_j)(x_i - y_j)^\top U_t$ for all $(i, j) \in [n] \times n$. This implies that the total number of arithmetic operations is $O(n^2dk)$. Therefore, the number of arithmetic operations at each loop is

$$\tilde{O} \left(n^2dk + dk^2 + k^3 + \frac{n^2 \|C\|_\infty^2}{\epsilon^2} \max \left\{ 1, \frac{\|C\|_\infty^2}{\epsilon^2} \right\} \right). \quad (3.17)$$

Putting Eq. (3.16) and Eq. (3.17) together with $k = \tilde{O}(1)$ yields the desired result. \square

Remark 3.9 Theorem 3.8 is surprising in that it provides a finite-time guarantee for finding an ϵ -stationary point of a nonsmooth function f over a nonconvex constraint set. This is impossible for general nonconvex nonsmooth optimization even in the Euclidean setting [Zhang et al., 2020, Shamir, 2020]. Our results demonstrate that the max-min optimization model in Eq. (2.1) has a special structure that makes fast computation possible.

Remark 3.10 Note that our algorithms only return an approximate stationary point for the nonconvex max-min optimization model in Eq. (2.1), which needs to be evaluated in practice. It is also interesting to compare such stationary point to the global optimal solution of computing the SRW distance. This is very challenging in general due to multiple stationary points of non-convex max-min optimization model in Eq. (2.1) but possible if the data has certain structure. We leave it to the future work.

4 Experiments

We conduct numerical experiments to evaluate the computation of the PRW distance by the RGAS and RAGAS algorithms. The baseline approaches include the computation of SRW distance with the Frank-Wolfe algorithm¹ [Paty and Cuturi, 2019] and the computation of Wasserstein distance with the POT software package² [Flamary and Courty, 2017]. For the RGAS and RAGAS algorithms, we set $\gamma = 0.01$ unless stated otherwise, $\beta = 0.8$ and $\alpha = 10^{-6}$. For the experiments on the MNIST digits, we run the feature extractor pretrained in PyTorch 1.5. All the experiments are implemented in Python 3.7 with Numpy 1.18 on a ThinkPad X1 with an Intel Core i7-10710U (6 cores and 12 threads) and 16GB memory, equipped with Ubuntu 20.04.

Fragmented hypercube. We conduct our first experiment on the fragmented hypercube which is also used to evaluate the SRW distance [Paty and Cuturi, 2019] and FactoredOT [Forrow et al., 2019]. In particular, we consider $\mu = \mathcal{U}([-1, 1]^d)$ which is an uniform distribution over an hypercube and $\nu = T_\# \mu$ which is the push-forward of μ under the map $T(x) = x + 2\text{sign}(x) \odot (\sum_{k=1}^{k^*} e_k)$. Note that

¹Available in <https://github.com/francois pierrepaty/SubspaceRobustWasserstein>.

²Available in <https://github.com/PythonOT/POT>

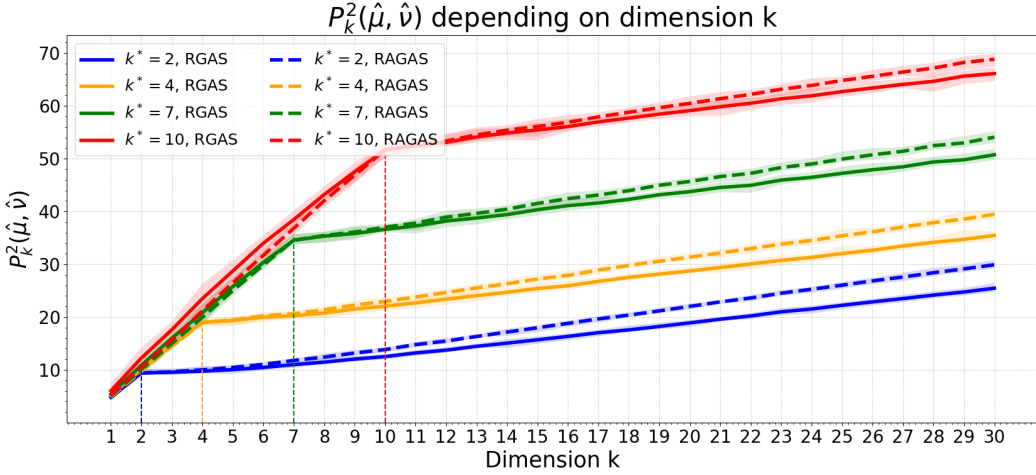


Figure 1: Computation of $\mathcal{P}_k^2(\hat{\mu}, \hat{\nu})$ depending on the dimension $k \in [d]$ and $k^* \in \{2, 4, 7, 10\}$, where $\hat{\mu}$ and $\hat{\nu}$ stand for the empirical measures of μ and ν with 100 points. The solid and dash curves are the computation of $\mathcal{P}_k^2(\hat{\mu}, \hat{\nu})$ with the RGAS and RAGAS algorithms, respectively. Each curve is the mean over 100 samples with shaded area covering the min and max values.

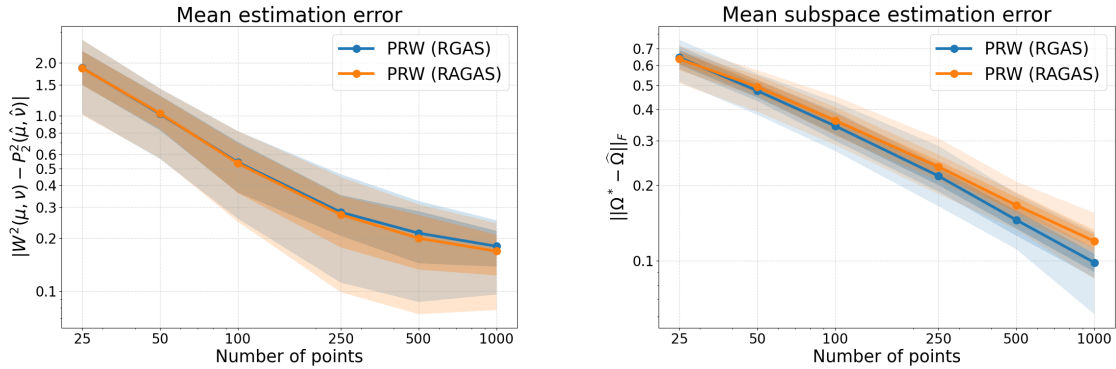


Figure 2: Mean estimation error (left) and mean subspace estimation error (right), with varying number of points n . The shaded areas represent the 10%-90% and 25%-75% quantiles over 100 samples.

$\text{sign}(\cdot)$ is taken element-wise, $k^* \in [d]$ and (e_1, \dots, e_d) is the canonical basis of \mathbb{R}^d . By the definition, T divides $[-1, 1]^d$ into four different hyper-rectangles, as well as serves as a subgradient of convex function. This together with Brenier's theorem (cf. [Villani \[2003, Theorem 2.12\]](#)) implies that T is an optimal transport map between μ and $\nu = T_{\#}\mu$ with $\mathcal{W}_2^2(\mu, \nu) = 4k^*$. Notice that the displacement vector $T(x) - x$ is optimal for any $x \in \mathbb{R}^d$ and always belongs to the k^* -dimensional subspace spanned by $\{e_j\}_{j \in [k^*]}$. Putting these pieces together yields that $\mathcal{P}_k^2(\mu, \nu) = 4k^*$ for any $k \geq k^*$.

Figure 1 presents the behavior of $\mathcal{P}_k^2(\hat{\mu}, \hat{\nu})$ as a function of $k^* \in \{2, 4, 7, 10\}$, where $\hat{\mu}$ and $\hat{\nu}$ are empirical distributions corresponding to μ and ν , respectively. The sequence is concave and increases slowly after $k = k^*$, which makes sense since the last $d - k^*$ dimensions only represent noise. The rigorous argument for the SRW distance is presented in [Paty and Cuturi \[2019, Proposition 3\]](#) but hard

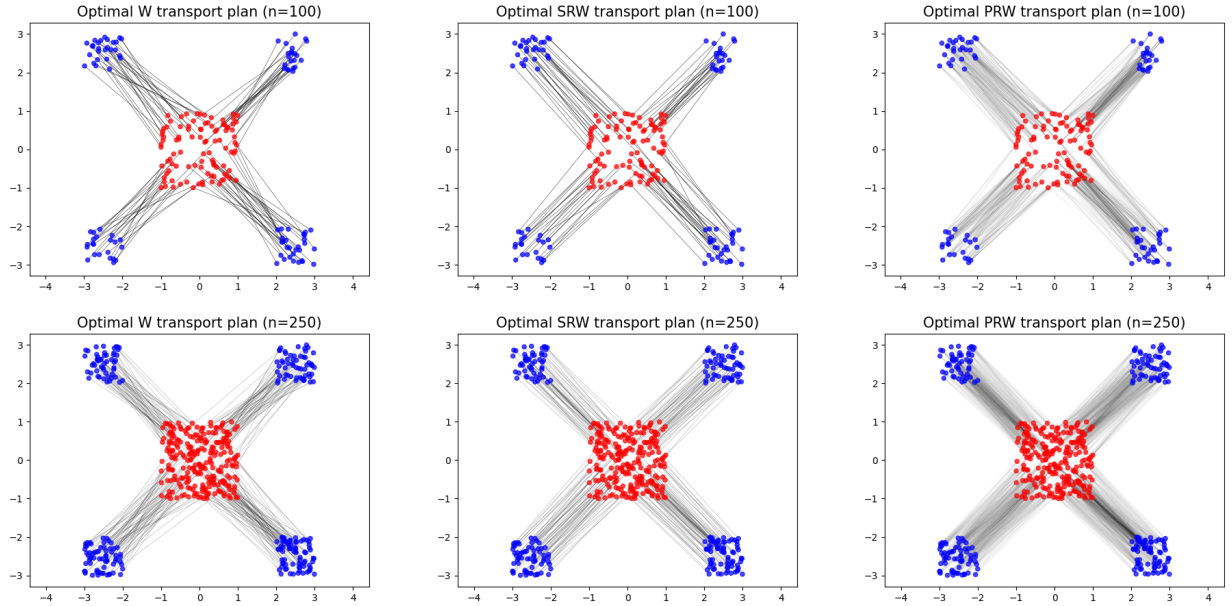


Figure 3: Fragmented hypercube with $(n, d) = (100, 30)$ (above) and $(n, d) = (250, 30)$ (bottom). Optimal mappings in the Wasserstein space (left), in the SRW space (middle) and the PRW space (right). Geodesics in the PRW space are robust to statistical noise.

to be extended here since the PRW distance can not be characterized as a sum of eigenvalues.

Figure 2 presents mean estimation error and mean subspace estimation error with varying number of points $n \in \{25, 50, 100, 250, 500, 1000\}$. In particular, \widehat{U} is an approximate optimal subspace projection achieved by computing $\mathcal{P}_k^2(\widehat{\mu}, \widehat{\nu})$ with our algorithms and Ω^* is the optimal projection matrix onto the k^* -dimensional subspace spanned by $\{e_j\}_{j \in [k^*]}$. We set $k^* = 2$ here and $\widehat{\mu}$ and $\widehat{\nu}$ are constructed from μ and ν respectively with n points each. The quality of solutions obtained by the RGAS and RAGAS algorithms are roughly the same.

Figure 3 presents the optimal transport plan in the Wasserstein space (left), the optimal transport plan in the SRW space (middle), and the optimal transport plan in the PRW space (right) between $\widehat{\mu}$ and $\widehat{\nu}$. We consider two cases: $n = 100$ and $n = 250$, in our experiment and observe that our results are consistent with [Paty and Cuturi \[2019, Figure 5\]](#), showing that both PRW and SRW distances share important properties with the Wasserstein distance.

Robustness of \mathcal{P}_k to noise. We conduct our second experiment on the Gaussian distribution³. In particular, we consider $\mu = \mathcal{N}(0, \Sigma_1)$ and $\nu = \mathcal{N}(0, \Sigma_2)$ where $\Sigma_1, \Sigma_2 \in \mathbb{R}^{d \times d}$ are positive semidefinite matrices of rank k^* . This implies that either of the support of μ and ν is the k^* -dimensional subspace of \mathbb{R}^d . Even though the supports of μ and ν can be different, their union is included in a $2k^*$ -dimensional subspace. Putting these pieces together yields that $\mathcal{P}_k^2(\mu, \nu) = \mathcal{W}_2^2(\mu, \nu)$ for any $k \geq 2k^*$. In our experiment, we set $d = 20$ and sample 100 independent couples of covariance matrices (Σ_1, Σ_2) , where

³ [Paty and Cuturi \[2019\]](#) conducted this experiment with their projected supergradient ascent algorithm (cf. [Paty and Cuturi \[2019, Algorithm 1\]](#)) with the EMD solver from the POT software package. For a fair comparison, we use Riemannian supergradient ascent algorithm (cf. Algorithm 3) with the EMD solver here; see Appendix for the details.

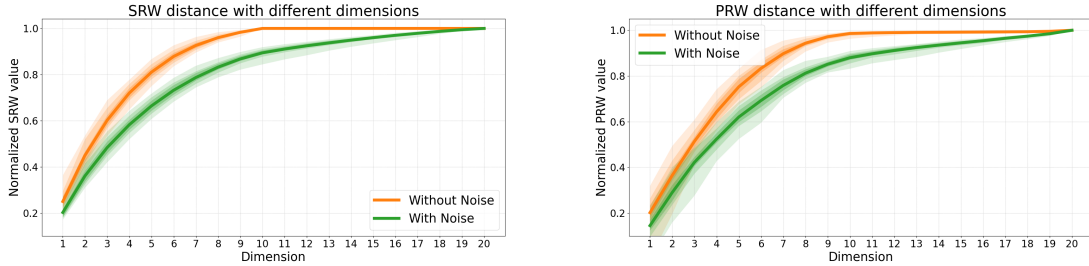


Figure 4: Mean normalized SRW distance (left) and mean normalized PRW distance (right) as a function of dimension. The shaded area shows the 10%-90% and 25%-75% quantiles over the 100 samples.

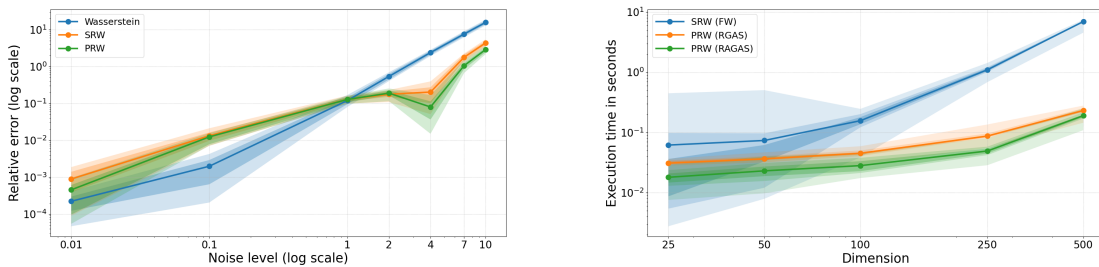


Figure 5: (Left) Comparison of mean relative errors over 100 samples, depending on the noise level. The shaded areas show the min-max values and the 10%-90% quantiles; (Right) Comparisons of mean computation times on CPU. The shaded areas show the minimum and maximum values over 50 runs.

each has independently a Wishart distribution with $k^* = 5$ degrees of freedom. Then we construct the empirical measures $\hat{\mu}$ and $\hat{\nu}$ by drawing $n = 100$ points from $\mathcal{N}(0, \Sigma_1)$ and $\mathcal{N}(0, \Sigma_2)$.

Figure 4 presents the mean value of $\mathcal{S}_k^2(\hat{\mu}, \hat{\nu})/\mathcal{W}_2^2(\hat{\mu}, \hat{\nu})$ (left) and $\mathcal{P}_k^2(\hat{\mu}, \hat{\nu})/\mathcal{W}_2^2(\hat{\mu}, \hat{\nu})$ (right) over 100 samples with varying k . We plot the curves for both noise-free and noisy data, where white noise ($\mathcal{N}(0, I_d)$) was added to each data point. With moderate noise, the data is approximately on two 5-dimensional subspaces and both the SRW and PRW distances do not vary too much. Our results are consistent with the SRW distance presented in [Paty and Cuturi \[2019, Figure 6\]](#), showing that the PRW distance is also robust to random perturbation of the data.

Figure 5 (left) presents the comparison of mean relative errors over 100 samples as the noise level varies. In particular, we construct the empirical measures $\hat{\mu}_\sigma$ and $\hat{\nu}_\sigma$ by gradually adding Gaussian noise $\sigma \mathcal{N}(0, I_d)$ to the points. The relative errors of the Wasserstein, SRW and PRW distances are defined the same as in [Paty and Cuturi \[2019, Section 6.3\]](#). For small noise level, the imprecision in the computation of the SRW distance adds to the error caused by the added noise, while the computation of the PRW distance with our algorithms is less sensitive to such noise. When the noise has the moderate to high variance, the PRW distance is the most robust to noise, followed by the SRW distance, both of which outperform the Wasserstein distance.

Computation time of algorithms. We conduct our third experiment on the fragmented hypercube with dimension $d \in \{25, 50, 100, 250, 500\}$, subspace dimension $k = 2$, number of points $n = 100$ and threshold $\epsilon = 0.001$. For the SRW and the PRW distances, the regularization parameter is set as $\eta = 0.2$

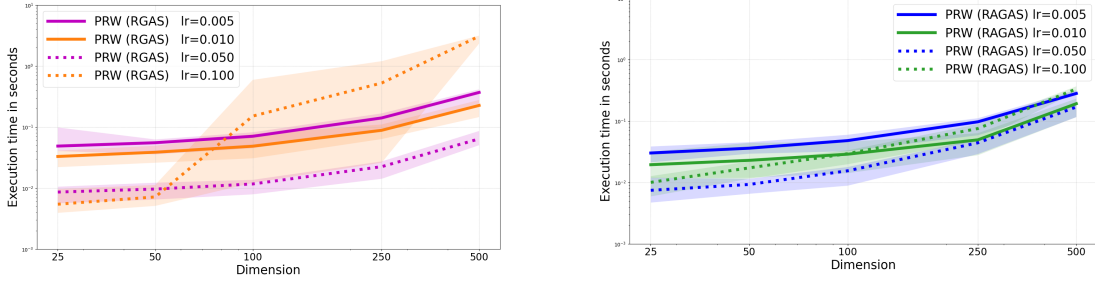


Figure 7: Comparisons of mean computation time of the RGAS and RAGAS algorithms on CPU (log-log scale) for different learning rates. The shaded areas show the max-min values over 50 runs.

for $n < 250$ and $\eta = 0.5$ otherwise⁴, as well as the scaling for the matrix C (cf. Definition 2.4) is applied for stabilizing the algorithms. We stop the RGAS and RAGAS algorithms when $\|U_{t+1} - U_t\|_F / \|U_t\|_F \leq \epsilon$.

Figure 5 (right) presents the mean computation time of the SRW distance with the Frank-Wolfe algorithm [Paty and Cuturi, 2019] and the PRW distance with our RGAS and RAGAS algorithms. Our approach is significantly faster since the complexity bound of their approach is quadratic in dimension d while our methods are linear in dimension d .

Robustness of algorithms to learning rate.

We conduct our fourth experiment on the fragmented hypercube to evaluate the robustness of our RGAS and RAGAS algorithms by choosing the learning rate $\gamma \in \{0.01, 0.1\}$. The parameter setting is the same as that in the third experiment.

Figure 6 indicates that the RAGAS algorithm is more robust than the RGAS algorithm as the learning rates varies, with smaller variance in computation time (seconds). This is the case especially when the dimension is large, showing the advantage of the adaptive strategies in practice.

To demonstrate the advantage of the adaptive strategies in practice, we initialize the learning rate using four options $\gamma \in \{0.005, 0.01, 0.05, 0.1\}$ and present the results for the RGAS and RAGAS algorithms separately in Figure 7. This is consistent with the results in Figure 6 and supports that the RAGAS algorithm is more robust than the RGAS algorithm to the learning rate.

Experiments on real data. We compute the PRW and SRW distances between all pairs of items in a corpus of seven *movie scripts*. Each script is tokenized to a list of words, which is transformed to a measure over \mathbb{R}^{300} using WORD2VEC [Mikolov et al., 2018] where each weight is word frequency. The SRW and PRW distances between all pairs of movies are in Table 1, which is consistent with the SRW distance in Paty and Cuturi [2019, Figure 9] and demonstrate that the PRW distance is smaller than SRW distance. We also compute the SRW and PRW for a preprocessed corpus of eight Shakespeare

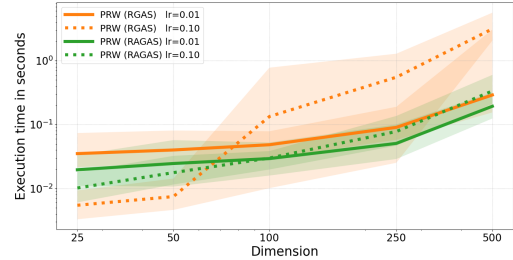


Figure 6: Comparisons of mean computation time of the RGAS and RAGAS algorithms on CPU (log-log scale) for different learning rates. The shaded areas show the max-min values over 50 runs.

using four options $\gamma \in \{0.005, 0.01, 0.05, 0.1\}$ and present the results for the RGAS and RAGAS algorithms separately in Figure 7. This is consistent with the results in Figure 6 and supports that the RAGAS algorithm is more robust than the RGAS algorithm to the learning rate.

⁴Available in <https://github.com/francoispierrepaty/SubspaceRobustWasserstein>

	D	G	I	KB1	KB2	TM	T
D	0/0	0.184/0.126	0.185/0.135	0.195/0.153	0.202/0.162	0.186/0.134	0.170/0.105
G	0.184/0.126	0/0	0.172/0.101	0.196/0.146	0.203/0.158	0.175/ 0.095	0.184/0.128
I	0.185/0.135	0.172/0.101	0/0	0.195/0.155	0.203/0.166	0.169/0.099	0.180/0.134
KB1	0.195/0.153	0.196/0.146	0.195/0.155	0/0	0.164/0.089	0.190/0.146	0.179/0.132
KB2	0.202/0.162	0.203/0.158	0.203/0.166	0.164/0.089	0/0	0.193/0.155	0.180/0.138
TM	0.186/0.134	0.175/ 0.095	0.169/0.099	0.190/0.146	0.193/0.155	0/0	0.182/0.136
T	0.170/0.105	0.184/0.128	0.180/0.134	0.179/0.132	0.180/0.138	0.182/0.136	0/0

Table 1: Each entry is $\mathcal{S}_k^2/\mathcal{P}_k^2$ distance between different movie scripts. D = Dunkirk, G = Gravity, I = Interstellar, KB1 = Kill Bill Vol.1, KB2 = Kill Bill Vol.2, TM = The Martian, T = Titanic.

	H5	H	JC	TMV	O	RJ
H5	0/0	0.222/0.155	0.230/0.163	0.228/0.166	0.227/0.170	0.311/0.272
H	0.222/0.155	0/0	0.224/0.163	0.221/0.159	0.220/0.153	0.323/0.264
JC	0.230/0.163	0.224/0.163	0/0	0.221/ 0.156	0.219/0.157	0.246/0.191
TMV	0.228/0.166	0.221/0.159	0.221/0.156	0/0	0.222/ 0.154	0.292/0.230
O	0.227/0.170	0.220/ 0.153	0.219/0.157	0.222/0.154	0/0	0.264/0.215
RJ	0.311/0.272	0.323/0.264	0.246/0.191	0.292/0.230	0.264/0.215	0/0

Table 2: Each entry is $\mathcal{S}_k^2/\mathcal{P}_k^2$ distance between different Shakespeare plays. H5 = Henry V, H = Hamlet, JC = Julius Caesar, TMV = The Merchant of Venice, O = Othello, RJ = Romeo and Juliet.

operas. The PRW distance is consistently smaller than the corresponding SRW distance; see Table 2. Figure 8 displays the projection of two measures associated with *Dunkirk* versus *Interstellar* (left) and *Julius Caesar* versus *The Merchant of Venice* (right) onto their optimal 2-dimensional projection.

To further show the versatility of SRW and PRW distances, we extract the features of different MNIST digits using a convolutional neural network (CNN) and compute the scaled SRW and PRW distances between all pairs of MNIST digits. In particular, we use an off-the-shelf PyTorch implementation⁵ and pretrain on MNIST with 98.6% classification accuracy on the test set. We extract the 128-dimensional features of each digit from the penultimate layer of the CNN. Since the MNIST test set contains 1000 images per digit, each digit is associated with a measure over \mathbb{R}^{128000} . Then we compute the optimal 2-dimensional projection distance of measures associated with each pair of two digital classes and divide each distance by 1000; see Table 3 for the details. The minimum SRW and PRW distances in each row is highlighted to indicate its most similar digital class of that row, which coincides with our intuitions. For example, D1 is sometimes confused with D7 (0.58/0.47), while D4 is often confused with D9 (0.49/0.38) in scribbles.

Summary. The PRW distance has less discriminative power than the SRW distance which is equivalent to the Wasserstein distance [Paty and Cuturi, 2019, Proposition 2]. Such equivalence implies that the SRW distance suffers from the curse of dimensionality in theory. In contrast, the PRW distance has much better sample complexity than the SRW distance if the distributions satisfy the mild condition [Niles-Weed and Rigollet, 2019, Lin et al., 2020]. Our empirical evaluation shows that the PRW distance is computationally favorable and more robust than the SRW and Wasserstein distance, when the noise has the moderate to high variance.

⁵<https://github.com/pytorch/examples/blob/master/mnist/main.py>

	D0	D1	D2	D3	D4	D5	D6	D7	D8	D9
D0	0/0	0.97/0.79	0.80/0.59	1.20/0.92	1.23/0.90	1.03/0.71	0.81/0.59	0.86/0.66	1.06/0.79	1.09/0.81
D1	0.97/0.79	0/0	0.66/0.51	0.86/0.72	0.68/0.54	0.84/0.70	0.80/0.66	0.58/0.47	0.88/0.71	0.85/0.72
D2	0.80/0.59	0.66/0.51	0/0	0.73/0.54	1.08/0.79	1.08/0.83	0.90/0.70	0.70/0.53	0.68/0.52	1.07/0.81
D3	1.20/0.92	0.86/0.72	0.73/0.54	0/0	1.20/0.87	0.58/0.43	1.23/0.91	0.72/0.55	0.88/0.64	0.83/0.65
D4	1.23/0.90	0.68/0.54	1.08/0.79	1.20/0.87	0/0	1.00/0.75	0.85/0.62	0.79/0.61	1.09/0.78	0.49/0.38
D5	1.03/0.71	0.84/0.70	1.08/0.83	0.58/0.43	1.00/0.75	0/0	0.72/0.51	0.91/0.68	0.72/0.53	0.78/0.59
D6	0.81/0.59	0.80/0.66	0.90/0.70	1.23/0.91	0.85/0.62	0.72/0.51	0/0	1.11/0.83	0.92/0.66	1.22/0.83
D7	0.86/0.66	0.58/0.47	0.70/0.53	0.72/0.55	0.79/0.61	0.91/0.68	1.11/0.83	0/0	1.07/0.78	0.62/0.46
D8	1.06/0.79	0.88/0.71	0.68/0.52	0.88/0.64	1.09/0.78	0.72/0.53	0.92/0.66	1.07/0.78	0/0	0.87/0.63
D9	1.09/0.81	0.85/0.72	1.07/0.81	0.83/0.65	0.49/0.38	0.78/0.59	1.22/0.83	0.62/0.46	0.87/0.63	0/0

Table 3: Each entry is scaled $\mathcal{S}_k^2/\mathcal{P}_k^2$ distance between different hand-written digits.

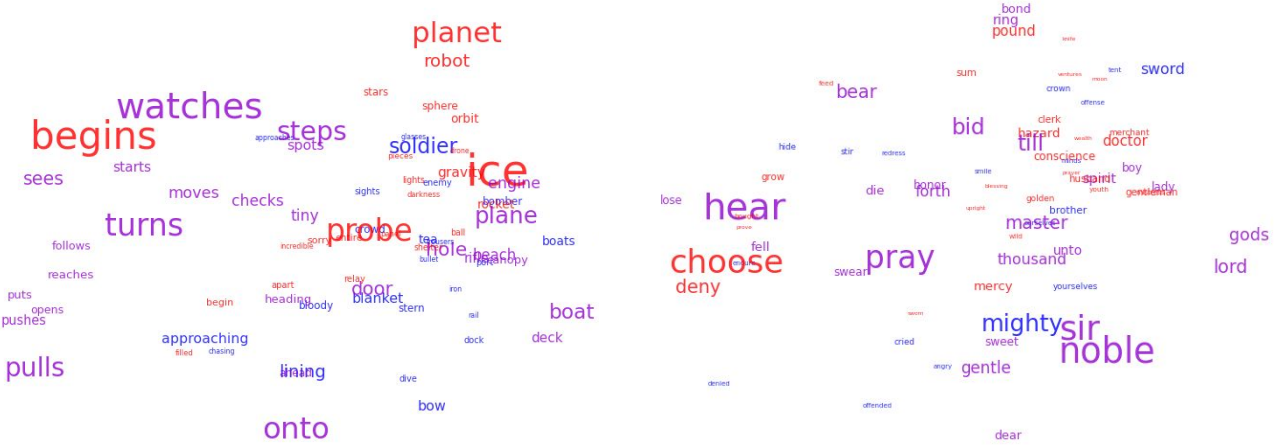


Figure 8: Optimal 2-dimensional projections between “Dunkirk” and “Interstellar” (left) and optimal 2-dimensional projections between “Julius Caesar” and “The Merchant of Venice” (right). Common words of two items are displayed in violet and the 30 most frequent words of each item are displayed.

5 Conclusion

We study in this paper the computation of the projection robust Wasserstein (PRW) distance in the discrete setting. A set of algorithms are developed for computing the entropic regularized PRW distance and both guaranteed to converge to an approximate pair of optimal subspace projection and optimal transportation plan. Experiments on synthetic and real datasets demonstrate that our approach to computing the PRW distance is an improvement over existing approaches based on the convex relaxation of the PRW distance and the Frank-Wolfe algorithm. Future work includes the theory for continuous distributions and applications of PRW distance to deep generative models.

6 Acknowledgements

This work was supported in part by the Mathematical Data Science program of the Office of Naval Research under grant number N00014-18-1-2764.

References

P-A. Absil and S. Hosseini. A collection of nonsmooth Riemannian optimization problems. In *Nonsmooth Optimization and Its Applications*, pages 1–15. Springer, 2019. (Cited on pages 5 and 31.)

P-A. Absil, R. Mahony, and R. Sepulchre. *Optimization Algorithms on Matrix Manifolds*. Princeton University Press, 2009. (Cited on pages 2, 6, and 31.)

J. Altschuler, J. Niles-Weed, and P. Rigollet. Near-linear time approximation algorithms for optimal transport via Sinkhorn iteration. In *NeurIPS*, pages 1964–1974, 2017. (Cited on pages 3 and 9.)

M. Arjovsky, S. Chintala, and L. Bottou. Wasserstein generative adversarial networks. In *ICML*, pages 214–223, 2017. (Cited on pages 1 and 2.)

G. Becigneul and O-E. Ganea. Riemannian adaptive optimization methods. In *ICLR*, 2019. (Cited on page 31.)

M. G. Bellemare, W. Dabney, and R. Munos. A distributional perspective on reinforcement learning. In *ICML*, pages 449–458, 2017. (Cited on page 1.)

G. C. Bento, O. P. Ferreira, and J. G. Melo. Iteration-complexity of gradient, subgradient and proximal point methods on Riemannian manifolds. *Journal of Optimization Theory and Applications*, 173(2):548–562, 2017. (Cited on page 31.)

E. Bernton. Langevin Monte Carlo and JKO splitting. In *COLT*, pages 1777–1798, 2018. (Cited on page 1.)

R. Bhatia, T. Jain, and Y. Lim. On the Bures-Wasserstein distance between positive definite matrices. *Expositiones Mathematicae*, 2018. (Cited on page 2.)

R. L. Bishop and B. O’Neill. Manifolds of negative curvature. *Transactions of the American Mathematical Society*, 145:1–49, 1969. (Cited on page 31.)

M. Blondel, V. Seguy, and A. Rolet. Smooth and sparse optimal transport. In *AISTATS*, pages 880–889, 2018. (Cited on pages 2 and 11.)

S. Bonnabel. Stochastic gradient descent on riemannian manifolds. *IEEE Transactions on Automatic Control*, 58(9):2217–2229, 2013. (Cited on page 31.)

N. Bonneel, M. Van De Panne, S. Paris, and W. Heidrich. Displacement interpolation using lagrangian mass transport. In *Proceedings of the 2011 SIGGRAPH Asia Conference*, pages 1–12, 2011. (Cited on page 37.)

N. Bonneel, J. Rabin, G. Peyré, and H. Pfister. Sliced and radon Wasserstein barycenters of measures. *Journal of Mathematical Imaging and Vision*, 51(1):22–45, 2015. (Cited on page 2.)

W. M. Boothby. *An Introduction to Differentiable Manifolds and Riemannian Geometry*. Academic Press, 1986. (Cited on page 6.)

N. Boumal, P-A. Absil, and C. Cartis. Global rates of convergence for nonconvex optimization on manifolds. *IMA Journal of Numerical Analysis*, 39(1):1–33, 2019. (Cited on pages 2, 7, and 31.)

G. Canas and L. Rosasco. Learning probability measures with respect to optimal transport metrics. In *NIPS*, pages 2492–2500, 2012. (Cited on page 2.)

S. Chen, S. Ma, A. M-C. So, and T. Zhang. Proximal gradient method for nonsmooth optimization over the Stiefel manifold. *SIAM Journal on Optimization*, 30(1):210–239, 2020. (Cited on pages 2, 7, and 31.)

Y. Chen, T. T. Georgiou, and A. Tannenbaum. Optimal transport for Gaussian mixture models. *IEEE Access*, 7:6269–6278, 2018. (Cited on page 2.)

X. Cheng, N. S. Chatterji, P. L. Bartlett, and M. I. Jordan. Underdamped Langevin MCMC: A non-asymptotic analysis. In *COLT*, pages 300–323, 2018. (Cited on page 1.)

N. Courty, R. Flamary, D. Tuia, and A. Rakotomamonjy. Optimal transport for domain adaptation. *IEEE Transactions on Pattern Analysis and Machine Intelligence*, 39(9):1853–1865, 2017. (Cited on page 1.)

C. Criscitiello and N. Boumal. Efficiently escaping saddle points on manifolds. In *NeurIPS*, pages 5985–5995, 2019. (Cited on page 31.)

M. Cuturi and A. Doucet. Fast computation of Wasserstein barycenters. In *ICML*, pages 685–693, 2014. (Cited on page 2.)

Marco Cuturi. Sinkhorn distances: Lightspeed computation of optimal transport. In *NeurIPS*, pages 2292–2300, 2013. (Cited on pages 2 and 3.)

A. S. Dalalyan and A. Karagulyan. User-friendly guarantees for the Langevin Monte Carlo with inaccurate gradient. *Stochastic Processes and their Applications*, 129(12):5278–5311, 2019. (Cited on page 1.)

K. Damian, B. Comm, and M. Garret. *The minimum cost flow problem and the network simplex method*. PhD thesis, Ph. D. Dissertation, Dissertation de Mastere, Université College Gublin, Irlande, 1991. (Cited on page 37.)

D. Davis and D. Drusvyatskiy. Stochastic model-based minimization of weakly convex functions. *SIAM Journal on Optimization*, 29(1):207–239, 2019. (Cited on pages 31 and 33.)

A. Dessein, N. Papadakis, and J-L. Rouas. Regularized optimal transport and the rot mover’s distance. *The Journal of Machine Learning Research*, 19(1):590–642, 2018. (Cited on pages 2 and 11.)

R. M. Dudley. The speed of mean Glivenko-Cantelli convergence. *The Annals of Mathematical Statistics*, 40(1):40–50, 1969. (Cited on page 2.)

P. Dvurechensky, A. Gasnikov, and A. Kroshnin. Computational optimal transport: Complexity by accelerated gradient descent is better than by Sinkhorn’s algorithm. In *ICML*, pages 1367–1376, 2018. (Cited on pages 3, 9, and 17.)

A. Edelman, T. A. Arias, and S. T. Smith. The geometry of algorithms with orthogonality constraints. *SIAM Journal on Matrix Analysis and Applications*, 20(2):303–353, 1998. (Cited on page 7.)

O. P. Ferreira and P. R. Oliveira. Subgradient algorithm on Riemannian manifolds. *Journal of Optimization Theory and Applications*, 97(1):93–104, 1998. (Cited on page 31.)

O. P. Ferreira and P. R. Oliveira. Proximal point algorithm on Riemannian manifolds. *Optimization*, 51(2):257–270, 2002. (Cited on page 31.)

R. Flamary and N. Courty. Pot python optimal transport library, 2017. URL <https://github.com/rflamary/POT>. (Cited on pages 18, 33, and 37.)

A. Forrow, J-C. Hütter, M. Nitzan, P. Rigollet, G. Schiebinger, and J. Weed. Statistical optimal transport via factored couplings. In *AISTATS*, pages 2454–2465, 2019. (Cited on pages 2 and 18.)

N. Fournier and A. Guillin. On the rate of convergence in Wasserstein distance of the empirical measure. *Probability Theory and Related Fields*, 162(3-4):707–738, 2015. (Cited on page 2.)

B. Gao, X. Liu, X. Chen, and Y. Yuan. A new first-order algorithmic framework for optimization problems with orthogonality constraints. *SIAM Journal on Optimization*, 28(1):302–332, 2018. (Cited on page 31.)

A. Genevay, G. Peyré, and M. Cuturi. Learning generative models with Sinkhorn divergences. In *AISTATS*, pages 1608–1617, 2018a. (Cited on page 1.)

A. Genevay, G. Peyré, and M. Cuturi. Learning generative models with Sinkhorn divergences. In *AISTATS*, pages 1608–1617, 2018b. (Cited on page 1.)

A. Genevay, L. Chizat, F. Bach, M. Cuturi, and G. Peyré. Sample complexity of Sinkhorn divergences. In *AISTATS*, pages 1574–1583, 2019. (Cited on page 2.)

S. Guminov, P. Dvurechensky, N. Tupitsa, and A. Gasnikov. Accelerated alternating minimization, accelerated Sinkhorn’s algorithm and accelerated iterative Bregman projections. *ArXiv Preprint: 1906.03622*, 2019. (Cited on page 3.)

N. Ho and L. Nguyen. Convergence rates of parameter estimation for some weakly identifiable finite mixtures. *Annals of Statistics*, 44(6):2726–2755, 2016. (Cited on page 1.)

N. Ho, X. Nguyen, M. Yurochkin, H. H. Bui, V. Huynh, and D. Phung. Multilevel clustering via Wasserstein means. In *ICML*, pages 1501–1509, 2017. (Cited on page 1.)

J. Hu, A. Milzarek, Z. Wen, and Y. Yuan. Adaptive quadratically regularized newton method for Riemannian optimization. *SIAM Journal on Matrix Analysis and Applications*, 39(3):1181–1207, 2018. (Cited on page 31.)

J. Hu, B. Jiang, L. Lin, Z. Wen, and Y. Yuan. Structured quasi-Newton methods for optimization with orthogonality constraints. *SIAM Journal on Scientific Computing*, 41(4):A2239–A2269, 2019. (Cited on page 31.)

H. Janati, T. Bazeille, B. Thirion, M. Cuturi, and A. Gramfort. Multi-subject MEG/EEG source imaging with sparse multi-task regression. *NeuroImage*, page 116847, 2020. (Cited on page 1.)

H. Kasai and B. Mishra. Inexact trust-region algorithms on riemannian manifolds. In *NeurIPS*, pages 4249–4260, 2018. (Cited on page 31.)

H. Kasai, P. Jawanpuria, and B. Mishra. Riemannian adaptive stochastic gradient algorithms on matrix manifolds. In *ICML*, pages 3262–3271, 2019. (Cited on page 2.)

S. Kolouri, K. Nadjahi, U. Simsekli, R. Badeau, and G. Rohde. Generalized sliced Wasserstein distances. In *NeurIPS*, pages 261–272, 2019. (Cited on page 2.)

J. Lei. Convergence and concentration of empirical measures under Wasserstein distance in unbounded functional spaces. *Bernoulli*, 26(1):767–798, 2020. (Cited on page 2.)

X. Li, S. Chen, Z. Deng, Q. Qu, Z. Zhu, and A. M-C. So. Nonsmooth optimization over Stiefel manifold: Riemannian subgradient methods. *ArXiv Preprint: 1911.05047*, 2019. (Cited on pages 31, 32, 33, and 35.)

T. Lin, N. Ho, and M. Jordan. On efficient optimal transport: An analysis of greedy and accelerated mirror descent algorithms. In *ICML*, pages 3982–3991, 2019a. (Cited on pages 3 and 17.)

T. Lin, N. Ho, and M. I. Jordan. On the efficiency of the Sinkhorn and Greenkhorn algorithms and their acceleration for optimal transport. *ArXiv Preprint: 1906.01437*, 2019b. (Cited on page 3.)

T. Lin, Z. Hu, and X. Guo. Sparsemax and relaxed wasserstein for topic sparsity. In *WSDM*, pages 141–149, 2019c. (Cited on page 1.)

T. Lin, Z. Zheng, E. Y. Chen, M. Cuturi, and M. I. Jordan. On projection robust optimal transport: Sample complexity and model misspecification. *ArXiv Preprint: 2006.12301*, 2020. (Cited on pages 2 and 23.)

H. Liu, A. M-C. So, and W. Wu. Quadratic optimization with orthogonality constraint: explicit Łojasiewicz exponent and linear convergence of retraction-based line-search and stochastic variance-reduced gradient methods. *Mathematical Programming*, 178(1-2):215–262, 2019. (Cited on pages 7 and 31.)

G. Mena and J. Niles-Weed. Statistical bounds for entropic optimal transport: sample complexity and the central limit theorem. In *NeurIPS*, pages 4543–4553, 2019. (Cited on page 2.)

T. Mikolov, E. Grave, P. Bojanowski, C. Puhrsch, and A. Joulin. Advances in pretraining distributed word representations. In *LREC*, 2018. (Cited on page 22.)

W. Mou, Y-A. Ma, M. J. Wainwright, P. L. Bartlett, and M. I. Jordan. High-order Langevin diffusion yields an accelerated MCMC algorithm. *ArXiv Preprint: 1908.10859*, 2019. (Cited on page 1.)

K. G. Murty and S. N. Kabadi. Some NP-complete problems in quadratic and nonlinear programming. *Mathematical Programming: Series A and B*, 39(2):117–129, 1987. (Cited on page 5.)

B. Muzellec and M. Cuturi. Generalizing point embeddings using the Wasserstein space of elliptical distributions. In *NIPS*, pages 10237–10248, 2018. (Cited on page 2.)

D. Nagaraj, P. Jain, and P. Netrapalli. SGD without replacement: sharper rates for general smooth convex functions. In *ICML*, pages 4703–4711, 2019. (Cited on page 1.)

K. Nguyen, N. Ho, T. Pham, and H. Bui. Distributional sliced-Wasserstein and applications to generative modeling. *ArXiv Preprint: 2002.07367*, 2020. (Cited on page 2.)

J. Niles-Weed and P. Rigollet. Estimation of Wasserstein distances in the spiked transport model. *ArXiv Preprint: 1909.07513*, 2019. (Cited on pages 1, 2, and 23.)

F-P. Paty and M. Cuturi. Subspace robust Wasserstein distances. In *ICML*, pages 5072–5081, 2019. (Cited on pages 2, 4, 5, 18, 19, 20, 21, 22, and 23.)

G. Peyré and M. Cuturi. Computational optimal transport. *Foundations and Trends® in Machine Learning*, 11(5-6):355–607, 2019. (Cited on page 1.)

J. Rabin, G. Peyré, J. Delon, and M. Bernot. Wasserstein barycenter and its application to texture mixing. In *International Conference on Scale Space and Variational Methods in Computer Vision*, pages 435–446. Springer, 2011. (Cited on page 2.)

R. T. Rockafellar. *Convex Analysis*, volume 36. Princeton University Press, 2015. (Cited on pages 8, 9, and 10.)

A. Rolet, M. Cuturi, and G. Peyré. Fast dictionary learning with a smoothed Wasserstein loss. In *AISTATS*, pages 630–638, 2016. (Cited on page 1.)

T. Salimans, H. Zhang, A. Radford, and D. Metaxas. Improving GANs using optimal transport. In *ICLR*, 2018. URL <https://openreview.net/forum?id=rkQkBnJAb>. (Cited on page 1.)

G. Schiebinger, J. Shu, M. Tabaka, B. Cleary, V. Subramanian, A. Solomon, J. Gould, S. Liu, S. Lin, and P. Berube. Optimal-transport analysis of single-cell gene expression identifies developmental trajectories in reprogramming. *Cell*, 176(4):928–943, 2019. (Cited on page 1.)

M. A. Schmitz, M. Heitz, N. Bonneel, F. Ngole, D. Coeurjolly, M. Cuturi, G. Peyré, and J-L. Starck. Wasserstein dictionary learning: Optimal transport-based unsupervised nonlinear dictionary learning. *SIAM Journal on Imaging Sciences*, 11(1):643–678, 2018. (Cited on page 1.)

O. Shamir. Can we find near-approximately-stationary points of nonsmooth nonconvex functions? *ArXiv Preprint: 2002.11962*, 2020. (Cited on page 18.)

S. Shirdhonkar and D. W. Jacobs. Approximate earth mover’s distance in linear time. In *CVPR*, pages 1–8. IEEE, 2008. (Cited on page 2.)

M. Sion. On general minimax theorems. *Pacific Journal of Mathematics*, 8(1):171–176, 1958. (Cited on page 5.)

S. Srivastava, V. Cevher, Q. Dinh, and D. Dunson. WASP: Scalable Bayes via barycenters of subset posteriors. In *AISTATS*, pages 912–920, 2015. (Cited on page 1.)

Y. Sun, N. Flammarion, and M. Fazel. Escaping from saddle points on Riemannian manifolds. In *NeurIPS*, pages 7274–7284, 2019. (Cited on page 31.)

R. E. Tarjan. Dynamic trees as search trees via euler tours, applied to the network simplex algorithm. *Mathematical Programming*, 78(2):169–177, 1997. (Cited on page 37.)

I. Tolstikhin, O. Bousquet, S. Gelly, and B. Schoelkopf. Wasserstein auto-encoders. In *ICLR*, 2018. (Cited on page 1.)

N. Tripuraneni, N. Flammarion, F. Bach, and M. I. Jordan. Averaging stochastic gradient descent on Riemannian manifolds. In *COLT*, pages 650–687, 2018. (Cited on page 31.)

J-P. Vial. Strong and weak convexity of sets and functions. *Mathematics of Operations Research*, 8(2):231–259, 1983. (Cited on pages 8 and 9.)

C. Villani. *Topics in Optimal Transportation*, volume 58. American Mathematical Soc., 2003. (Cited on pages 1 and 19.)

C. Villani. *Optimal Transport: Old and New*, volume 338. Springer Science & Business Media, 2008. (Cited on pages 1 and 4.)

J. Weed and F. Bach. Sharp asymptotic and finite-sample rates of convergence of empirical measures in Wasserstein distance. *Bernoulli*, 25(4A):2620–2648, 2019. (Cited on page 2.)

Z. Wen and W. Yin. A feasible method for optimization with orthogonality constraints. *Mathematical Programming*, 142(1-2):397–434, 2013. (Cited on pages 7 and 31.)

K. D. Yang, K. Damodaran, S. Venkatachalam, A. Soylemezoglu, G. V. Shivashankar, and C. Uhler. Predicting cell lineages using autoencoders and optimal transport. *PLoS Computational Biology*, 16(4):e1007828, 2020. (Cited on page 1.)

W. H. Yang, L-H. Zhang, and R. Song. Optimality conditions for the nonlinear programming problems on Riemannian manifolds. *Pacific Journal of Optimization*, 10(2):415–434, 2014. (Cited on page 9.)

H. Zhang and S. Sra. First-order methods for geodesically convex optimization. In *COLT*, pages 1617–1638, 2016. (Cited on page 31.)

H. Zhang, S. J. Reddi, and S. Sra. Riemannian SVRG: Fast stochastic optimization on Riemannian manifolds. In *NeurIPS*, pages 4592–4600, 2016. (Cited on page 31.)

J. Zhang, S. Ma, and S. Zhang. Primal-dual optimization algorithms over Riemannian manifolds: an iteration complexity analysis. *Mathematical Programming*, pages 1–46, 2019. (Cited on page 31.)

J. Zhang, H. Lin, S. Sra, and A. Jadbabaie. On complexity of finding stationary points of nonsmooth nonconvex functions. *ArXiv Preprint: 2002.04130*, 2020. (Cited on page 18.)

A Further Background Materials on Riemannian Optimization

The problem of optimizing a smooth function over the Riemannian manifold has been the subject of a large literature. [Absil et al. \[2009\]](#) provide a comprehensive treatment, showing how first-order and second-order algorithms are extended to the Riemannian setting and proving asymptotic convergence to first-order stationary points. [Boumal et al. \[2019\]](#) have established global sublinear convergence results for Riemannian gradient descent and Riemannian trust region algorithms, and further showed that the latter approach converges to a second order stationary point in polynomial time; see also [Kasai and Mishra \[2018\]](#), [Hu et al. \[2018, 2019\]](#). In contradistinction to the Euclidean setting, the Riemannian trust region algorithm requires a Hessian oracle. There have been also several recent papers on problem-specific algorithms [[Wen and Yin, 2013](#), [Gao et al., 2018](#), [Liu et al., 2019](#)] and primal-dual algorithms [[Zhang et al., 2019](#)] for Riemannian optimization.

Compared to the smooth setting, Riemannian nonsmooth optimization is harder and relatively less explored [[Absil and Hosseini, 2019](#)]. There are two main lines of work. In the first category, one considers optimizing geodesically convex function over a Riemannian manifold with subgradient-type algorithms; see, e.g., [Ferreira and Oliveira \[1998\]](#), [Zhang and Sra \[2016\]](#), [Bento et al. \[2017\]](#). In particular, [Ferreira and Oliveira \[1998\]](#) first established an asymptotic convergence result while [Zhang and Sra \[2016\]](#), [Bento et al. \[2017\]](#) derived a global convergence rate of $O(\epsilon^{-2})$ for the Riemannian subgradient algorithm. Unfortunately, these results are not useful for understanding the computation of the PRW distance in Eq. (2.1) since the Stiefel manifold is *compact* and every continuous and geodesically convex function on a compact Riemannian manifold must be a constant; see [Bishop and O’Neill \[1969, Proposition 2.2\]](#). In the second category, one assumes the tractable computation of the proximal mapping of the objective function over the Riemannian manifold. [Ferreira and Oliveira \[2002\]](#) proved that the Riemannian proximal point algorithm converges globally at a sublinear rate.

When specialized to the Stiefel manifold, [Chen et al. \[2020\]](#) consider the composite objective and proposed to compute the proximal mapping of nonsmooth component function over the tangent space. The resulting Riemannian proximal gradient algorithm is practical in real applications while achieving theoretical guarantees. [Li et al. \[2019\]](#) extended the results in [Davis and Drusvyatskiy \[2019\]](#) to the Riemannian setting and proposed a family of Riemannian subgradient-type methods for optimizing a weakly convex function over the Stiefel manifold. They also proved that their algorithms have an iteration complexity of $O(\epsilon^{-4})$ for driving a near-optimal stationarity measure below ϵ . Following up the direction proposed by [Li et al. \[2019\]](#), we derive a near-optimal condition (Definition B.1 and B.2) for the max-min optimization model in Eq. (2.2) and propose an algorithm with the finite-time convergence under this stationarity measure.

Finally, there are several results on stochastic optimization over the Riemannian manifold. [Bonnabel \[2013\]](#) proved the first asymptotic convergence result for Riemannian stochastic gradient descent, which is further extended by [Zhang et al. \[2016\]](#), [Tripuraneni et al. \[2018\]](#), [Becigneul and Ganea \[2019\]](#). If the Riemannian Hessian is not positive definite, a few recent works have developed frameworks to escape saddle points [[Sun et al., 2019](#), [Criscitiello and Boumal, 2019](#)].

B Near-Optimality Condition

In this section, we derive a near-optimal condition (Definition B.1 and B.2) for the max-min optimization model in Eq. (2.1) and the maximization of f over $\text{St}(d, k)$ in Eq. (2.4). Following [Davis and Drusvyatskiy \[2019\]](#), [Li et al. \[2019\]](#), we define the proximal mapping of f over $\text{St}(d, k)$ in Eq. (2.4),

which takes into account both the Stiefel manifold constraint and max-min structure⁶:

$$p(U) \in \operatorname{argmax}_{\bar{U} \in \operatorname{St}(d,k)} \{f(\bar{U}) - 6\|C\|_\infty \|\bar{U} - U\|_F^2\} \quad \text{for all } U \in \operatorname{St}(d,k).$$

After a simple calculation, we have

$$\Theta(U) := 12\|C\|_\infty \|p(U) - U\|_F \geq \operatorname{dist}(0, \operatorname{subdiff} f(\operatorname{prox}_{\rho f}(U))),$$

Therefore, we conclude from Definition 2.6 that $p(U) \in \operatorname{St}(d,k)$ is ϵ -approximate optimal subspace projection of f over $\operatorname{St}(d,k)$ in Eq. (2.4) if $\Theta(U) \leq \epsilon$. We remark that $\Theta(\bullet)$ is a well-defined surrogate stationarity measure of f over $\operatorname{St}(d,k)$ in Eq. (2.4). Indeed, if $\Theta(U) = 0$, then $U \in \operatorname{St}(d,k)$ is an optimal subspace projection. This inspires the following ϵ -near-optimality condition for any $\hat{U} \in \operatorname{St}(d,k)$.

Definition B.1 *A subspace projection $\hat{U} \in \operatorname{St}(d,k)$ is called an ϵ -approximate near-optimal subspace projection of f over $\operatorname{St}(d,k)$ in Eq. (2.4) if it satisfies $\Theta(\hat{U}) \leq \epsilon$.*

Equipped with Definition 2.2 and B.1, we define an ϵ -approximate pair of near-optimal subspace projection and optimal transportation plan for the computation of the PRW distance in Eq. (2.1).

Definition B.2 *The pair of subspace projection and transportation plan $(\hat{U}, \hat{\pi}) \in \operatorname{St}(d,k) \times \Pi(\mu, \nu)$ is an ϵ -approximate pair of near-optimal subspace projection and optimal transportation plan for the computation of the PRW distance in Eq. (2.1) if the following statements hold true:*

- \hat{U} is an ϵ -approximate near-optimal subspace projection of f over $\operatorname{St}(d,k)$ in Eq. (2.4).
- $\hat{\pi}$ is an ϵ -approximate optimal transportation plan for the subspace projection \hat{U} .

Finally, we prove that the stationary measure in Definition B.2 is a local surrogate for the stationary measure in Definition 2.7 in the following proposition.

Proposition B.1 *If $(U, \pi) \in \operatorname{St}(d,k) \times \Pi(\mu, \nu)$ is an ϵ -approximate pair of optimal subspace projection and optimal transportation plan of problem (2.1), it is an 3ϵ -approximate pair of optimal subspace projection and optimal transportation plan.*

Proof. By the definition, $(U, \pi) \in \operatorname{St}(d,k) \times \Pi(\mu, \nu)$ satisfies that π is an ϵ -approximate optimal transportation plan for the subspace projection U . Thus, it suffices to show that $\Theta(U) \leq 3\epsilon$. By the definition of $p(U)$, we have

$$f(p(U)) - 6\|C\|_\infty \|p(U) - U\|_F^2 \geq f(U).$$

Since f is $2\|C\|_\infty$ -weakly concave and each element of the subdifferential $\partial f(U)$ is bounded by $2\|C\|_\infty$ for all $U \in \operatorname{St}(d,k)$, the Riemannian subgradient inequality [Li et al., 2019, Theorem 1] implies that

$$f(\operatorname{prox}_{\rho f}(U)) - f(U) \leq \langle \xi, \operatorname{prox}_{\rho f}(U) - U \rangle + 2\|C\|_\infty \|\operatorname{prox}_{\rho f}(U) - U\|^2 \quad \text{for any } \xi \in \operatorname{subdiff} f(U).$$

Since $\operatorname{dist}(0, \operatorname{subdiff} f(U)) \leq \epsilon$, we have

$$f(\operatorname{prox}_{\rho f}(U)) - f(U) \leq \epsilon \|\operatorname{prox}_{\rho f}(U) - U\|_F + 2\|C\|_\infty \|\operatorname{prox}_{\rho f}(U) - U\|^2.$$

Putting these pieces together with the definition of $\Theta(U)$ yields the desired result. \square

⁶The proximal mapping $p(U)$ must exist since the Stiefel manifold is compact, yet may not be uniquely defined. However, this does not matter since $p(U)$ only appears in the analysis for the purpose of defining the surrogate stationarity measure; see Li et al. [2019].

Algorithm 3 Riemannian SuperGradient Ascent with Network Simplex Iteration (RSGAN)

- 1: **Input:** measures $\{(x_i, r_i)\}_{i \in [n]}$ and $\{(y_j, c_j)\}_{j \in [n]}$, dimension $k = \tilde{O}(1)$ and tolerance ϵ .
- 2: **Initialize:** $U_0 \in \text{St}(d, k)$, $\hat{\epsilon} \leftarrow \min\{\epsilon, \frac{\epsilon^2}{200\|C\|_\infty}\}$ and $\gamma_0 \leftarrow \frac{1}{k\|C\|_\infty}$.
- 3: **for** $t = 0, 1, 2, \dots, T-1$ **do**
- 4: Compute $\pi_{t+1} \leftarrow \text{OT}(\{(x_i, r_i)\}_{i \in [n]}, \{(y_j, c_j)\}_{j \in [n]}, U_t, \hat{\epsilon})$.
- 5: Compute $\xi_{t+1} \leftarrow P_{\text{St}}(2V_{\pi_{t+1}}U_t)$.
- 6: Compute $\gamma_{t+1} \leftarrow \gamma_0/\sqrt{t+1}$.
- 7: Compute $U_{t+1} \leftarrow \text{Retr}_{U_t}(\gamma_{t+1}\xi_{t+1})$.
- 8: **end for**

C Riemannian Supergradient meets Network Simplex Iteration

In this section, we propose a new algorithm, named *Riemannian SuperGradient Ascent with Network simplex iteration* (RSGAN), for computing the PRW distance in Eq. (2.1). The iterates are guaranteed to converge to an ϵ -approximate pair of *near-optimal* subspace projection and optimal transportation plan (cf. Definition B.2). The complexity bound is $\tilde{O}(n^2(d+n)\epsilon^{-4})$ if $k = \tilde{O}(1)$.

C.1 Algorithmic scheme

We start with a brief overview of the Riemannian supergradient ascent algorithm for nonsmooth Stiefel optimization. Letting $F : \mathbb{R}^{d \times k} \rightarrow \mathbb{R}$ be a nonsmooth but weakly concave function, we consider

$$\max_{U \in \text{St}(d, k)} F(U).$$

A generic Riemannian supergradient ascent algorithm for solving this problem is given by

$$U_{t+1} \leftarrow \text{Retr}_{U_t}(\gamma_{t+1}\xi_{t+1}) \quad \text{for any } \xi_{t+1} \in \text{subdiff } F(U_t),$$

where $\text{subdiff } F(U_t)$ is Riemannian subdifferential of F at U_t and Retr is any retraction on $\text{St}(d, k)$. For the nonconvex nonsmooth optimization, the stepsize setting $\gamma_{t+1} = \gamma_0/\sqrt{t+1}$ is widely accepted in both theory and practice [Davis and Drusvyatskiy, 2019, Li et al., 2019].

By the definition of Riemannian subdifferential, ξ_t can be obtained by taking $\xi \in \partial F(U)$ and by setting $\xi_t = P_{\text{St}}(\xi)$. Thus, it is necessary for us to specify the subdifferential of f in Eq. (2.4). Using the symmetry of V_π , we have

$$\partial f(U) = \text{Conv} \left\{ 2V_{\pi^*}U \mid \pi^* \in \underset{\pi \in \Pi(\mu, \nu)}{\text{argmin}} \langle UU^\top, V_\pi \rangle \right\}, \quad \text{for any } U \in \mathbb{R}^{d \times k}.$$

The remaining step is to solve an OT problem with a given U at each inner loop of the maximization and use the output $\pi(U)$ to obtain an inexact supergradient of f . Since the OT problem with a given U is exactly an LP, this is possible and can be done by applying the variant of network simplex method in the POT package [Flamary and Courty, 2017]. While the simplex method can exactly solve this LP, we adopt the inexact solving rule as a practical matter. More specifically, the output π_{t+1} is an $\hat{\epsilon}$ -approximate optimal transportation plan (cf. Definition 2.2). With the inexact solving rule, the framework of regularized OT can be also adopted with the same scheme as presented in Section 3. To this end, we summarize the pseudocode of the RSGAN algorithm in Algorithm 3.

C.2 Complexity analysis for Algorithm 3

We define a function which is important to the subsequent analysis of Algorithm 3:

$$\Phi(U) := \max_{U' \in \text{St}(d, k)} \{f(U') - 6\|C\|_\infty\|U' - U\|_F^2\} \quad \text{for all } U \in \text{St}(d, k).$$

Our first lemma provides a key inequality for quantifying the progress of the iterates $\{(U^t, \pi^t)\}_{t \geq 1}$ generated by Algorithm 3 using $\Phi(\bullet)$ as the potential function.

Lemma C.1 *Letting $\{(U_t, \pi_t)\}_{t \geq 1}$ be the iterates generated by Algorithm 3, we have*

$$\begin{aligned} \Phi(U_{t+1}) &\geq \Phi(U_t) - 12\gamma_{t+1}\|C\|_\infty(f(U_t) - f(p(U_t)) + 4\|C\|_\infty\|p(U_t) - U_t\|_F^2 + \hat{\epsilon}) \\ &\quad - 200\gamma_{t+1}^2\|C\|_\infty^3(\gamma_{t+1}^2L_2^2\|C\|_\infty^2 + \gamma_{t+1}\|C\|_\infty + \sqrt{k}). \end{aligned}$$

Proof. Since $p(U_t) \in \text{St}(d, k)$, we have

$$\Phi(U_{t+1}) \geq f(p(U_t)) - 6\|C\|_\infty\|p(U_t) - U_{t+1}\|_F^2. \quad (\text{C.1})$$

Using the update formula of U_{t+1} , we have

$$\|p(U_t) - U_{t+1}\|_F^2 = \|p(U_t) - \text{Retr}_{U_t}(\gamma_{t+1}\xi_{t+1})\|_F^2.$$

Using the Cauchy-Schwarz inequality and Proposition 2.1, we have

$$\begin{aligned} &\|p(U_t) - \text{Retr}_{U_t}(\gamma_{t+1}\xi_{t+1})\|_F^2 \\ &= \|(U_t + \gamma_{t+1}\xi_{t+1} - p(U_t)) + (\text{Retr}_{U_t}(\gamma_{t+1}\xi_{t+1}) - U_t - \gamma_{t+1}\xi_{t+1})\|_F^2 \\ &\leq \|U_t + \gamma_{t+1}\xi_{t+1} - p(U_t)\|_F^2 + \|\text{Retr}_{U_t}(\gamma_{t+1}\xi_{t+1}) - (U_t + \gamma_{t+1}\xi_{t+1})\|_F^2 \\ &\quad + 2\|U_t + \gamma_{t+1}\xi_{t+1} - p(U_t)\|_F\|\text{Retr}_{U_t}(\gamma_{t+1}\xi_{t+1}) - (U_t + \gamma_{t+1}\xi_{t+1})\|_F \\ &\leq \|U_t + \gamma_{t+1}\xi_{t+1} - p(U_t)\|_F^2 + \gamma_{t+1}^4L_2^2\|\xi_{t+1}\|_F^4 + 2\gamma_{t+1}^2\|U_t + \gamma_{t+1}\xi_{t+1} - p(U_t)\|_F\|\xi_{t+1}\|_F^2 \\ &\leq \|U_t - p(U_t)\|_F^2 + 2\gamma_{t+1}\langle \xi_{t+1}, U_t - p(U_t) \rangle + \gamma_{t+1}^2\|\xi_{t+1}\|_F^2 + \gamma_{t+1}^4L_2^2\|\xi_{t+1}\|_F^4 \\ &\quad + 2\gamma_{t+1}^2\|U_t + \gamma_{t+1}\xi_{t+1} - p(U_t)\|_F\|\xi_{t+1}\|_F^2. \end{aligned}$$

Since $U_t \in \text{St}(d, k)$ and $p(U_t) \in \text{St}(d, k)$, we have $\|U_t\|_F \leq \sqrt{k}$ and $\|p(U_t)\|_F \leq \sqrt{k}$. By the update formula for ξ_{t+1} , we have

$$\|\xi_{t+1}\|_F = \|P_{\text{Tr}_{U_{t-1}}\text{St}}(2V_{\pi_{t+1}}U_t)\|_F \leq 2\|V_{\pi_{t+1}}U_t\|_F.$$

Since $U_t \in \text{St}(d, k)$ and $\pi_{t+1} \in \Pi(\mu, \nu)$, we have $\|\xi_{t+1}\|_F \leq 2\|C\|_\infty$. Putting all these pieces together yields that

$$\begin{aligned} \|p(U_t) - U_{t+1}\|_F^2 &\leq \|U_t - p(U_t)\|_F^2 + 2\gamma_{t+1}\langle \xi_{t+1}, U_t - p(U_t) \rangle + 4\gamma_{t+1}^2\|C\|_\infty^2 \\ &\quad + 16\gamma_{t+1}^4L_2^2\|C\|_\infty^4 + 16\gamma_{t+1}^3\|C\|_\infty^3 + 16\gamma_{t+1}^2\sqrt{k}\|C\|_\infty^2. \end{aligned} \quad (\text{C.2})$$

Plugging Eq. (C.2) into Eq. (C.1) and simplifying the inequality using $k \geq 1$, we have

$$\begin{aligned} \Phi(U_{t+1}) &\geq f(p(U_t)) - 6\|C\|_\infty\|U_t - p(U_t)\|_F^2 - 12\gamma_{t+1}\|C\|_\infty\langle \xi_{t+1}, U_t - p(U_t) \rangle \\ &\quad - 200\gamma_{t+1}^2\|C\|_\infty^3(\gamma_{t+1}^2L_2^2\|C\|_\infty^2 + \gamma_{t+1}\|C\|_\infty + \sqrt{k}). \end{aligned}$$

By the definition of $\Phi(\bullet)$ and $p(\bullet)$, we have

$$\begin{aligned}\Phi(U_{t+1}) &\geq \Phi(U_t) - 12\gamma_{t+1}\|C\|_\infty\langle\xi_{t+1}, U_t - p(U_t)\rangle \\ &\quad - 200\gamma_{t+1}^2\|C\|_\infty^3\left(\gamma_{t+1}^2L_2^2\|C\|_\infty^2 + \gamma_{t+1}\|C\|_\infty + \sqrt{k}\right).\end{aligned}\tag{C.3}$$

Now we proceed to bound the term $\langle\xi_{t+1}, U_t - p(U_t)\rangle$. Letting $\xi_t^* = P_{\text{Tr}_{U_t}\text{St}}(2V_{\pi_t^*}U_t)$ where π_t^* is a minimizer of unregularized OT problem, i.e., $\pi_t^* \in \arg\min_{\pi \in \Pi(\mu, \nu)} \langle U_t U_t^\top, V_\pi \rangle$, we have

$$\langle\xi_{t+1}, U_t - p(U_t)\rangle \leq \langle\xi_t^*, U_t - p(U_t)\rangle + \|\xi_{t+1} - \xi_t^*\|_F\|U_t - p(U_t)\|_F.\tag{C.4}$$

Since $f(U) = \min_{\pi \in \Pi(\mu, \nu)} \langle U_t U_t^\top, V_\pi \rangle$ is $2\|C\|_\infty$ -weakly concave over $\mathbb{R}^{d \times k}$ (cf. Lemma 2.2), $\xi_t^* \in$ subdiff $f(U_t)$ and each element in the subdifferential $\partial f(U)$ is bounded by $2\|C\|_\infty$ for all $U \in \text{St}(d, k)$ (cf. Lemma 2.3), the Riemannian subgradient inequality [Li et al., 2019, Theorem 1] holds true and implies that

$$f(p(U_t)) \leq f(U_t) + \langle\xi_t^*, p(U_t) - U_t\rangle + 2\|C\|_\infty\|p(U_t) - U_t\|_F^2.$$

This implies that

$$\langle\xi_t^*, U_t - p(U_t)\rangle \leq f(U_t) - f(p(U_t)) + 2\|C\|_\infty\|p(U_t) - U_t\|_F^2.\tag{C.5}$$

By the definition of ξ_{t+1} and ξ_t^* , we have

$$\|\xi_{t+1} - \xi_t^*\|_F^2 = \|P_{\text{Tr}_{U_t}\text{St}}(2V_{\pi_{t+1}}U_t) - P_{\text{Tr}_{U_t}\text{St}}(2V_{\pi_t^*}U_t)\|_F^2 \leq 4\|(V_{\pi_{t+1}} - V_{\pi_t^*})U_t\|_F^2.$$

By the definition of the subroutine $\text{OT}(\{(x_i, r_i)\}_{i \in [n]}, \{(y_j, c_j)\}_{j \in [n]}, U, \hat{\epsilon})$ in Algorithm 3, we have $\pi_{t+1} \in \Pi(\mu, \nu)$ and $0 \leq \langle U_t U_t^\top, V_{\pi_{t+1}} - V_{\pi_t^*} \rangle \leq \hat{\epsilon}$. This together with $\|V_{\pi_{t+1}} - V_{\pi_t^*}\|_F \leq 2\|C\|_\infty$ yield that

$$\|\xi_{t+1} - \xi_t^*\|_F^2 \leq 8\|C\|_\infty\hat{\epsilon}.$$

Using Young's inequality, we have

$$\begin{aligned}\|\xi_{t+1} - \xi_t^*\|_F\|U_t - p(U_t)\|_F &\leq \frac{\|\xi_{t+1} - \xi_t^*\|_F^2}{8\|C\|_\infty} + 2\|C\|_\infty\|U_t - p(U_t)\|_F^2 \\ &\leq \hat{\epsilon} + 2\|C\|_\infty\|U_t - p(U_t)\|_F^2.\end{aligned}\tag{C.6}$$

Combining Eq. (C.3), Eq. (C.4), Eq. (C.5) and Eq. (C.6) yields the desired result. \square

Putting Lemma C.1 together with the definition of $p(\bullet)$, we have the following consequence:

Proposition C.2 *Letting $\{(U_t, \pi_t)\}_{t \geq 1}$ be the iterates generated by Algorithm 3, we have*

$$\begin{aligned}&\frac{24\|C\|_\infty^2 \sum_{t=0}^{T-1} \gamma_{t+1}\|p(U_t) - U_t\|_F^2}{\sum_{t=0}^{T-1} \gamma_{t+1}} \\ &\leq \frac{\gamma_0^{-1}\Delta_\Phi + 200\gamma_0\|C\|_\infty^3(\gamma_0^2L_2^2\|C\|_\infty^2 + \gamma_0\|C\|_\infty + \sqrt{k}(\log(T) + 1))}{2\sqrt{T}} + 12\|C\|_\infty\hat{\epsilon},\end{aligned}$$

where $\Delta_\Phi = \max_{U \in \text{St}(d, k)} \Phi(U) - \Phi(U_0)$ is the initial objective gap.

Proof. By the definition of $p(\bullet)$, we have

$$\begin{aligned} & f(U_t) - f(p(U_t)) + 4\|C\|_\infty\|p(U_t) - U_t\|_F^2 \\ &= f(U_t) - (f(p(U_t)) - 6\|C\|_\infty\|p(U_t) - U_t\|_F^2) - 2\|C\|_\infty\|p(U_t) - U_t\|_F^2 \\ &\leq -2\|C\|_\infty\|p(U_t) - U_t\|_F^2. \end{aligned}$$

Using Lemma C.1, we have

$$\begin{aligned} \Phi(U_{t+1}) &\geq \Phi(U_t) + 24\gamma_{t+1}\|C\|_\infty^2\|p(U_t) - U_t\|_F^2 - 12\gamma_{t+1}\|C\|_\infty\widehat{\epsilon} \\ &\quad - 200\gamma_{t+1}^2\|C\|_\infty^3(\gamma_{t+1}^2L_2^2\|C\|_\infty^2 + \gamma_{t+1}\|C\|_\infty + \sqrt{k}). \end{aligned}$$

Rearranging this inequality, we have

$$\begin{aligned} 24\gamma_{t+1}\|C\|_\infty^2\|p(U_t) - U_t\|_F^2 &\leq \Phi(U_{t+1}) - \Phi(U_t) + 12\gamma_{t+1}\|C\|_\infty\widehat{\epsilon} \\ &\quad + 200\gamma_{t+1}^2\|C\|_\infty^3(\gamma_{t+1}^2L_2^2\|C\|_\infty^2 + \gamma_{t+1}\|C\|_\infty + \sqrt{k}). \end{aligned}$$

Summing up over $t = 0, 1, 2, \dots, T-1$ yields that

$$\frac{24\|C\|_\infty^2 \sum_{t=0}^{T-1} \gamma_{t+1}\|p(U_t) - U_t\|_F^2}{\sum_{t=0}^{T-1} \gamma_{t+1}} \leq \frac{\Delta\Phi + 200\|C\|_\infty^3(\sum_{t=1}^T \gamma_t^2(\gamma_t^2L_2^2\|C\|_\infty^2 + \gamma_t\|C\|_\infty + \sqrt{k}))}{2\sum_{t=1}^T \gamma_t} + 12\|C\|_\infty\widehat{\epsilon}.$$

By the definition of $\{\gamma_t\}_{t \geq 1}$, we have

$$\sum_{t=1}^T \gamma_t \geq \gamma_0\sqrt{T}, \quad \sum_{t=1}^T \gamma_t^2 \leq \gamma_0^2(\log(T) + 1), \quad \sum_{t=1}^T \gamma_t^3 \leq 3\gamma_0^3, \quad \sum_{t=1}^T \gamma_t^4 \leq 2\gamma_0^4.$$

Putting these pieces together yields the desired result. \square

We proceed to provide an upper bound for the number of iterations needed to return an ϵ -approximate near-optimal subspace projection $U_t \in \text{St}(d, k)$ satisfying $\Theta(U_t) \leq \epsilon$ in Algorithm 3.

Theorem C.3 *Letting $\{(U_t, \pi_t)\}_{t \geq 1}$ be the iterates generated by Algorithm 3, the number of iterations required to reach $\Theta(U_t) \leq \epsilon$ satisfies*

$$t = \tilde{O}\left(\frac{k^2\|C\|_\infty^4}{\epsilon^4}\right).$$

Proof. By the definition of $\Theta(\bullet)$ and $p(\bullet)$, we have

$$\Theta(U_t) = 12\|C\|_\infty\|p(U_t) - U_t\|_F.$$

Using Proposition C.2, we have

$$\frac{\sum_{t=0}^{T-1} \gamma_{t+1}(\Theta(U_t))^2}{\sum_{t=0}^{T-1} \gamma_{t+1}} \leq \frac{3\gamma_0^{-1}\Delta\Phi + 600\gamma_0\|C\|_\infty^3(\gamma_0^2L_2^2\|C\|_\infty^2 + \gamma_0\|C\|_\infty + \sqrt{k}(\log(T) + 1))}{\sqrt{T}} + 72\|C\|_\infty\widehat{\epsilon}.$$

Furthermore, by the definition $\Phi(\bullet)$, we have

$$\begin{aligned} |\Phi(U)| &\leq \max_{U' \in \text{St}(d, k)} |f(U') + 6\|C\|_\infty\|U' - U\|_F^2| \\ &\leq \max_{U \in \text{St}(d, k)} \max_{U' \in \text{St}(d, k)} |f(U') + 6\|C\|_\infty\|U' - U\|_F^2| \\ &\leq \max_{U \in \text{St}(d, k)} |f(U)| + 12k\|C\|_\infty. \end{aligned}$$

By the definition of $f(\bullet)$, we have $\max_{U \in \text{St}(d,k)} |f(U)| \leq \|C\|_\infty$. Putting these pieces together with $k \geq 1$ implies that $|\Phi(U)| \leq 20k\|C\|_\infty$. By the definition of Δ_Φ , we conclude that $\Delta_\Phi \leq 40k\|C\|_\infty$. Given that $\hat{\epsilon} \leq \epsilon^2/144\|C\|_\infty$, $\gamma_0 = 1/\|C\|_\infty$ and $\Theta(U_t) > \epsilon$ for all $t = 0, 1, \dots, T-1$, the upper bound T must satisfy

$$\epsilon^2 \leq \frac{240k\|C\|_\infty^2 + 1200\|C\|_\infty^2(L_2^2 + \sqrt{k}\log(T) + \sqrt{k} + 1)}{\sqrt{T}}.$$

This implies the desired result. \square

Equipped with Theorem C.3 and Algorithm 3, we establish the complexity bound of Algorithm 3.

Theorem C.4 *The RSGAN algorithm (cf. Algorithm 3) returns an ϵ -approximate pair of near-optimal subspace projection and optimal transportation plan of computing the PRW distance in Eq. (2.1) (cf. Definition B.2) in*

$$\tilde{O}\left(\frac{n^2(n+d)\|C\|_\infty^4}{\epsilon^4}\right)$$

arithmetic operations.

Proof. First, Theorem C.3 implies that the iteration complexity of Algorithm 3 is

$$\tilde{O}\left(\frac{k^2\|C\|_\infty^4}{\epsilon^4}\right). \quad (\text{C.7})$$

This implies that U_t is an ϵ -approximate near-optimal subspace projection of problem (2.4). Furthermore, $\hat{\epsilon} = \min\{\epsilon, \epsilon^2/144\|C\|_\infty\}$. Since $\pi_{t+1} \leftarrow \text{OT}(\{(x_i, r_i)\}_{i \in [n]}, \{(y_j, c_j)\}_{j \in [n]}, U_t, \hat{\epsilon})$, we have $\pi_{t+1} \in \Pi(\mu, \nu)$ and $\langle U_t U_t^\top, V_{\pi_{t+1}} - V_{\pi_t^*} \rangle \leq \hat{\epsilon} \leq \epsilon$. This implies that π_{t+1} is an ϵ -approximate optimal transportation plan for the subspace projection U_t . Therefore, we conclude that $(U_t, \pi_{t+1}) \in \text{St}(d, k) \times \Pi(\mu, \nu)$ is an ϵ -approximate pair of near-optimal subspace projection and optimal transportation plan of problem (2.1).

The remaining step is to analyze the complexity bound. Note that the most of software packages, e.g., POT [Flamary and Courty, 2017], implement the OT subroutine using a variant of the network simplex method with a block search pivoting strategy [Damian et al., 1991, Bonneel et al., 2011]. The best known complexity bound is provided in Tarjan [1997] and is $\tilde{O}(n^3)$. Using the same argument in Theorem 3.8, the number of arithmetic operations at each loop is

$$\tilde{O}(n^2dk + dk^2 + k^3 + n^3). \quad (\text{C.8})$$

Putting Eq. (C.7) and Eq. (C.8) together with $k = \tilde{O}(1)$ yields the desired result. \square

Remark C.5 *The complexity bound of Algorithm 3 is better than that of Algorithm 1 and 2 in terms of ϵ and $\|C\|_\infty$. This makes sense since Algorithm 3 only returns an ϵ -approximate pair of near-optimal subspace projection and optimal transportation plan which is weaker than an ϵ -approximate pair of optimal subspace projection and optimal transportation plan. Furthermore, Algorithm 3 implements the network simplex method as the inner loop which might suffer when n is large and yield unstable performance in practice.*